UNIVERSIDADE DE LISBOA
FACULDADE DE CIÊNCIAS
DEPARTAMENTO DE FÍSICA

Increased Fall Risk Evaluation in the Elderly: A Video-based Approach for Gait Analysis

Sara Viveiros Ponte

Mestrado Integrado em Engenharia Biomédica e Biofísica
Perfil em Engenharia Clínica e Instrumentação Médica

Dissertação orientada por:

Dr. Luís Ducla Soares, Instituto Universitário de Lisboa (ISCTE-IUL)
Dr. Nuno Matela, Faculdade de Ciências da Universidade de Lisboa (FCUL)

2021

“Nothing in life is to be feared, it is only to be understood. Now is the time to understand more, so that we may fear less.”

- Marie Curie

Abstract

Worldwide, falls are a major public health problem. Their risk assessment occurs predominantly in clinical environments, having a great dependency on the healthcare professionals who perform the evaluation. Hence, the aim of this thesis was to develop a quantitative and objective approach to assess fall risk through two-dimensional (2D) video gait analysis. Data was acquired from two groups with antagonistic risk evaluations, a control group and an elderly group with increased fall risk, during two separate activities: walking and a standard Time Up and Go (TUG) test. The video sequences acquired were further pre-processed with the purpose of obtaining human skeletons for each frame of the video, followed by the computation of gait and time parameters for both activities. The estimated time parameters by the developed algorithm for the walking activity were compared with those estimated by the gait analysis *Contemplas* software, and the mean difference measured among both systems ranged between 0s and 0.02s. In addition, automatically extracted TUG time parameters were validated with those manually extracted for every TUG test video, and they proved to be strongly correlated (rho > 0.8). The same parameters were also in agreement with a study from the literature with similar characteristics, in which the TUG phases duration estimated were within the same range of the study. Furthermore, a Wilcoxon Rank Sum test was conducted to determine how well a given parameter could distinguish between young and elderly groups, and results showed a total of 15 out of 22 discriminant parameters (ρ-value < 0.05), with a greater representation of TUG time parameters (9/15). Apart from video capture, personal information such as age, sex, weight, height, history of falls, use of walking aid and presence of motor diseases were also acquired, and a Pearson correlation was computed between this supplementary data and the fall risk binary evaluation for each subject. This correlation revealed a strong linear relationship between age and increased fall risk, corroborated with a coefficient of 0.98. Results demonstrated that the developed algorithm was able to detect differences between people who had or not risk of falling, providing promising fall risk indicators that could contribute to a more objective and detailed evaluation of fall risk.

Keywords: quantitative fall risk assessment, video gait analysis, 2D skeletons, elderly people, timed up and go

Resumo

Uma em cada três pessoas com idade igual ou superior a 65 anos cai, pelo menos, uma vez por ano. Esta incidência, faz das quedas a segunda maior causa de morte acidental, e no caso do idoso, é o tipo de acidente doméstico que mais frequentemente acontece. A população mais afetada é a faixa etária acima dos 65 anos, que se caracteriza por reunir um conjunto de fatores que advêm da idade, e que, de certa forma, a predispõe para este tipo de ocorrência. Com o envelhecimento, advêm maiores dificuldades ao nível motor, muscular e visual, que tornam a população idosa mais vulnerável no momento anterior à queda. A maioria destas quedas acarreta custos, tanto a nível financeiro como psicológico, que podem influenciar diretamente a qualidade de vida destes sujeitos. Deste modo, prevenir a queda em pessoas idosas significa também atuar na prevenção de perda de autonomia, independência e bem estar. A persistência de altas taxas de quedas tornou este tema num problema de saúde pública, e que, por essa razão, urge o desenvolvimento de estratégias preventivas que ajudem a mitigar a ocorrência de quedas e as suas consequências.

Uma das formas de atuar preventivamente à ocorrência destes episódios passa pela monitorização do risco de queda de cada indivíduo. Tradicionalmente, a monitorização pode ser realizada por um fisioterapeuta e utilizar como ferramentas de apoio ao diagnóstico escalas, questionários e/ou testes funcionais. No entanto, esta abordagem de avaliação de risco tende a ser limitativa, quer pela sua subjetividade inerente e pela dependência ao clínico que a realiza, quer também pelo facto de certos indicadores de risco de queda não serem facilmente identificados a olho nu. Por conseguinte, novos métodos tecnológicos estão a ser cada vez mais desenvolvidos com o intuito de aceder à condição clínica de pessoas idosas de uma forma mais objetiva.

Neste sentido, o objetivo da presente tese é desenvolver um algoritmo capaz de avaliar quantitativamente o risco de queda na população idosa, com a inclusão de captura e análise de vídeo durante a marcha. Com a definição deste objetivo, será possível recolher informação adicional à adquirida por parte de um fisioterapeuta, e, portanto, permitir que a avaliação final seja o mais informada possível para que novas opções de tratamento sejam adaptadas ao risco de cada indivíduo. Deste modo, poderá ser melhorada a atual avaliação clínica, com influência na redução do risco de queda e nas suas futuras consequências.

Com este propósito, realizaram-se duas fases de aquisições de dados em parceria com a Escola Superior da Cruz Vermelha Portuguesa de Lisboa, cada fase ocupada com um diferente grupo de sujeitos. Numa fase inicial, a recolha de dados contou com cerca de 29 jovens adultos saudáveis que integraram o grupo de controlo deste estudo; numa segunda fase, foram recolhidos dados de 14 idosos. Durante os dois períodos de aquisição, foi pedido aos participantes que executassem dois tipos de atividades — marcha e o teste Timed up and Go (TUG) — e durante a execução das mesmas, foi instalada uma câmara de vídeo que capturou o movimento dos sujeitos durante as duas atividades. Para além da captura de vídeo, recolheu-se informação demográfica e associada a risco de queda através de um questionário. O grupo de idosos foi também sujeito a uma avaliação binária de risco de queda por parte dos fisioterapeutas

através de uma escala denominada de Fall Risk Questionnaire (FRQ), que se resumiu a uma avaliação de risco a todos os idosos incluídos no estudo (n=6).

Posteriormente à primeira fase de recolhas, os vídeos para cada uma das atividades foram submetidos a um processo de pré-processamento, que consistiu na obtenção de esqueletos para cada um dos tramas constituintes do vídeo através do software OpenPose. O OpenPose recebe como entrada um dos vídeos recolhidos e converte, no mesmo formato, um vídeo com o movimento do participante representado por um esqueleto, trama a trama. Terminada esta tarefa, os tramas foram convertidos para imagens binárias. O processamento dos dados foi desenvolvido na íntegra em MATLAB, e traduziu-se em calcular parâmetros espaço-temporais e parâmetros de postura para as sequências de vídeo da atividade da marcha, e parâmetros temporais para as sequências do teste TUG.

Inicialmente, os parâmetros temporais (gait cycle time, stance time, double support time, pre-swing time) computados para as sequências de marcha do grupo de controlo foram validados por comparação com os medidos com o software Contemplas. Trata-se de um software desenhado para análise de marcha num contexto clínico, e este passo foi delineado com o objetivo de verificar que os parâmetros obtidos por um algoritmo desenvolvido em MATLAB iam de encontro com os estimados por um software já validado. Tendo em consideração que a análise no Contemplas integrava uma parte manual feita pelo fisioterapeuta, foi definida uma margem de erro de 1 trama, e com isso, definido um intervalo de incerteza. Se o valor do parâmetro estivesse contido no intervalo definido era contado como um caso correto. De forma a comparar os resultados dos parâmetros para os dois sistemas (algoritmo e *Contemplas*), calculou-se exatidão e diferenças de médias para cada parâmetro entre os dois sistemas. Os resultados revelam exatidões entre 87% e 94% e diferenças na média na ordem dos centésimos de segundo, que corroboram que o algoritmo proposto pode estimar, em média, e para um determinado grupo de sujeitos, parâmetros muito próximos dos estimados por um software já validado no contexto clínico. Estes resultados ajudam também a sustentar a hipótese que o desenvolvimento de um algoritmo automático e funcional pode ser o equivalente a um sistema mais caro que necessita intervenção manual para a análise.

Numa fase seguinte, os parâmetros temporais obtidos para o grupo de controlo nas sequências do teste TUG foram também submetidos a um processo de validação. Neste caso, a validação dividiu-se em duas etapas: i) validação manual e ii) validação com um estudo da literatura. Para a primeira, compararam-se duas formas de estimar parâmetros, uma de forma manual que incluiu uma análise individual vídeo a vídeo através da divisão do TUG em diferentes fases (sit-stand, walk, turn-around, stand-sit), e a automática realizada através do algoritmo desenvolvido em MATLAB. Comparam-se os valores obtidos para cada uma das fases nas duas abordagens utilizadas e obteve-se coeficientes de correlação acima de 0.8, com diferenças de média a variar entre 0.01s e 0.02s. Na segunda etapa de validação, os valores temporais obtidos para as fases do teste TUG foram também comparados com os obtidos num estudo da literatura com características semelhantes. Posto isto, verificou-se que a duração das fases do TUG estimada para o grupo de controlo estava dentro do mesmo intervalo que a estimada para um estudo cujos participantes também eram jovens adultos saudáveis. Ambas as etapas de validação não só sugerem que o algoritmo proposto garante parâmetros de confiança para o teste TUG, como também permite a computação automática da duração do teste e de outros parâmetros que não são usualmente medidos pelos fisioterapeutas durante um teste regular.

A última fase foi ocupada com a computação de parâmetros para os dois grupos de participantes — controlo e idosos —, cujo objetivo foi verificar quão bem um determinado parâmetro era capaz de distinguir entre um grupo com e sem risco de queda. Para cada um dos 22 parâmetros, fez-se o teste estatístico Wilcoxon Rank Sum. Considerou-se que o parâmetro era significativamente diferente entre os dois grupos para um p-value abaixo de 0.05. Dos 22 testes realizados, resultaram 15 parâmetros significativos,

com uma maior incidência nos parâmetros obtidos para o teste TUG. Esta incidência indica a utilidade do teste TUG para diferenciar dois grupos com avaliações de risco antagónicas. Adicionalmente, a duração estimada do teste TUG para o grupo de idosos (=16.67s) está de acordo com um estudo publicado pela BMC Geriatrics que revela que uma duração superior a 13.5s pode ser um indicativo de risco de queda. Os resultados da comparação dos dois grupos de risco expressam a capacidade do algoritmo identificar parâmetros que poderão funcionar como indicadores de risco de queda, uma vez que revelam alterações na marcha, na postura e na execução de determinadas tarefas.

Por último, foi calculado uma correlação de Pearson entre a informação adquirida através do questionário e a avaliação de risco para cada grupo de sujeitos. A idade mostrou-se fortemente correlacionada com o risco de queda, com a obtenção de uma correlação de 0.98.

A presente tese teve como objetivo principal o desenvolvimento de um sistema capaz de aceder quantitativamente ao risco de queda na população idosa. Com esse propósito, foram computados automaticamente parâmetros temporais e de marcha para cada uma das duas atividades, cujas métricas deram bons indicativos de futuros indicadores de risco de queda. A maioria destes parâmetros não são normalmente medidos durante uma avaliação clínica, e por essa razão, o sistema proposto é uma forma de quantificar a análise observacional do fisioterapeuta. Desta forma, é também possível fornecer informação mais detalhada, com a finalidade de oferecer opções de tratamento mais indicadas para cada indivíduo, para que no futuro as quedas possam vir a ser evitadas.

Palavras chave: avaliação de risco de queda, análise de marcha em vídeo, esqueletos em 2D, idosos, teste TUG

Acknowledgements

Em primeiro lugar, gostaria de agradecer aos meus dois orientadores, que me acompanharam ao longo deste último ano, ao prof. Nuno Matela, da Faculdade de Ciências da Universidade de Lisboa, e ao prof. Luís Ducla Soares, do Instituto de Telecomunicações; pelo apoio incessante, pela disponibilidade e acessibilidade que sempre tiveram para comigo, por todas as críticas construtivas e pela esperança inesgotável que depositaram neste projeto, apesar de todas as suas contrariedades.

Em segundo lugar, gostaria de agradecer aos fisioterapeutas da Escola Superior de Saúde da Cruz Vermelha Portuguesa de Lisboa, em especial ao fisioterapeuta Tiago Atalaia, por ter sido o primeiro contacto e um dos principais responsáveis pela idealização do tema desta dissertação, e ao fisioterapeuta Rodrigo Martins, por todo o tempo que dedicou a este projeto e pela contribuição importante que teve na sua concretização.

Gostaria de também agradecer a todos os participantes que integraram este estudo, e que de certa forma, o tornaram possível, em concreto ao grupo de estudantes de fisioterapia da ESSCVP e ao grupo de idosos residentes do Casal Ventoso.

Um especial agradecimento a quem contribuiu para este projeto na sua fase inicial, ao prof. Paulo Correia, por ver o copo sempre meio cheio, e ao Pedro e ao Tanmay pelos trabalhos que desenvolveram anteriormente, e pela ajuda que foram para o desenvolvimento desta dissertação.

Não poderia deixar de agradecer aos meus amigos da faculdade, que me acolheram nestes últimos 5 anos e que me dividem o coração entre Lisboa-Açores. Sem eles, o meu percurso académico não faria sentido. Em especial, ao João; pelo apoio constante, pela companhia diária, por me incentivar a acreditar mais em mim e por me fazer sair da minha zona de conforto e ver o mundo de outra forma.

E, sem faltar, às minhas amigas de sempre, que mesmo distantes, fizeram-se por estar sempre presentes.

Por último, mas não menos importante, à minha família. Aos meus pais que de tudo fizeram para me dar uma melhor educação, e que, sem eles, este percurso nunca seria possível. Ao Nuno e à Sandra, por terem sido a minha segunda casa. E aos meus avós, pelo amor incondicional e pela sorte que é ainda tê-los ao meu lado.

Table of Contents

List of Figures

List of Tables

List of Abbreviations

2D Two Dimensional

3D Three Dimensional

BMI Body Mass Index

BoS Base of Support

CNS Central Nervous System

CoG Center of Gravity

CV Coefficient of Variation

EMG Electromyography

ESSCVP Escola Superior de Saúde da Cruz Vermelha Portuguesa

FF Flat Foot

fps Frames Per Second

FRQ Fall Risk Questionnaire

GEI Gait Energy Image

GMM Gaussian Mixture Model

GRF Ground Reaction Forces

GTI Gait Texture Image

HS Heel Strike

IC Initial Contact

IMU Inertial Measurement Unit

MOCAP Motion Capture

PNS Peripheral Nervous System

RGB Red Green Blue

SGEI Skeleton Gait Energy Image

List of Abbreviations

STD Standard Deviation

SVM Support Vector Machines

TO Toe Off

TOR Torso Orientation

TUG Timed Up and Go

Chapter 1

Introduction

In this chapter, the motivation for the development of a quantitative fall risk evaluation system is presented (see Section 1.1). Section 1.2, 1.3 and 1.4 are dedicated, respectively, to enumerating the main objectives and the major contributions of this thesis, and to explaining its structure.

1.1 Motivation

According to the World Health Organization, it is estimated that 646 000 fatal falls occur each year around the world, making it the second most common cause of accidental death [1]. With the aging of the population, it is expected that both the number of falls and their severity increase. In fact, statistics show that the age group over 65 years old is the most affected, with one out of three people falling at least once a year [2]. One of the reasons behind this high incidence might be explained by the fact that increasing age also increases the chances of developing neurological disorders or other classes of pathologies that can affect gait and posture, thus influencing the ability to remain steadily balanced and avoid falling.

Regarding non-fatal falls, each year around 37.3 million people require medical and hospital care [3], involving costs that not everyone can afford to pay. Fall injuries are among the 20 most expensive injuries to treat [4], with the U.S. average hospital cost [5] per fall injury being over $30.000.

Apart from financial costs, there are also emotional and psychological consequences for someone who has experienced a fall. The impact of a fall can be significant at a personal level, as it may lead to a withdrawal from daily life activities, subsequent social isolation due to fear of falling and loss of confidence, and then depression [4]. This is particularly true among elderly fallers, since 50% of them are unable to get up after a fall [2]. As a result of this incapacity to live independently, either caregivers or nursing home care become necessary.

The persistence of high fall rates in the elderly population over the years has turned this into a major public health problem, because of the resultant injuries and consequences for the affected individuals, as well as the huge costs to the healthcare system. If preventive measures are not taken in the immediate future, the number of injuries caused by falls is projected to be 100% higher in 2030 [6]. Hence, there is an urgent need for developing cost-effective preventive strategies that help mitigate the occurrence of falls and their consequences, since existing systems are mainly focused on detecting falls, with little emphasis on fall prediction.

Traditional strategies rely mostly on assessing and monitoring elderly people in a clinical environment, using as evaluation tool either functional tests to assess gait or/and posture or specific screening forms to assess fall risk factors. In both cases, the naked eye observation of physiotherapists plays an important role on the evaluation. However, due to the subjectivity and little accuracy that are inherent to this

form of assessment, more technological and quantitative approaches using vision-based or sensor-based systems have started to be developed.

Following this trend, this thesis set out to improve quantitatively the current methodology used by physiotherapists to assess risk of falling and to provide additional information to their evaluation. Helping clinicians identify fall risk indicators can lead to better informed personalized interventions for their patients, thus improving fall risk assessment and reducing chances of falling and its associated complications.

1.2 Objectives

The main goal of this thesis is to develop an objective method to quantify the fall risk evaluation done by physiotherapists in the elderly, with the proposed method relying on acquired 2D video to perform gait analysis during two activities: i) Walking and ii) Timed Up and Go test. To achieve this aim, the following more specific objectives were defined:

- Validate temporal gait features extracted from the walking sequences with a software designed to perform gait analysis in a clinical context;
- Validate temporal features extracted from the execution of Timed Up and Go (TUG) test; and
- Identify parameters that could be used as fall risk indicators in elderly populations.

1.3 Major Contributions

This thesis focuses on the development of an algorithm in MATLAB, a low-cost approach and easy to set up, in which fall risk could be quantitatively assessed. Its main contributions can be enumerated as follows:

- Automatic and less expensive estimation of temporal gait parameters from 2D skeletons during walking such as gait cycle time, stance time, double support time and pre-swing time; analogous to the ones measured using *Contemplas* software for gait analysis;
- Automatic estimation of temporal parameters from 2D skeletons during the execution of TUG test such as sit-stand time, turn-around time, stand-sit time, walk time and TUG time; analogous to the manual measurement; and
- Identification of temporal and gait parameters that can work as fall risk indicators to assess fall risk in the elderly;

1.4 Thesis Structure

This thesis is organized in six chapters. Chapter 1, which corresponds to the current chapter, briefly introduces the context and motivation for this thesis, along with the corresponding objectives, contributions and structure. Chapter 2 presents the fundamentals of gait analysis and their relation with falls. Chapter 3 focuses on providing a literature review on the existing approaches to assess fall risk in elderly people, ranging from the most traditional to the most recent methods. This review is centered mainly in solutions that rely on 2D video gait analysis. Chapter 4 describes the primary methods applied to

pre-process and analyze the acquired 2D video dataset to evaluate fall risk in the elderly, as well as the material used for their development. Chapter 5 presents the experiments and results of the fall risk evaluation system. Finally, Chapter 6 concludes this thesis with a summary of the achievements of this work and also gives some suggestions for future work.

Chapter 2

Background: Falls and Gait Analysis

In this chapter, the fundamentals of gait analysis and its relation with falls are discussed. Section 2.1 explains why falls occur and their main risk factors. Section 2.2 presents the existing systems to prevent falls, with focus on automatic fall detection and fall prediction systems. Section 2.3 introduces the main concepts of gait by providing theoretical context about steady human locomotion. Section 2.4 describes the common systems to perform gait analysis. Finally, Section 2.5 summarizes the standard architecture of a gait analysis system.

2.1 Falls and Risk Factors

A fall is defined as an event that results in a person coming to rest inadvertently on the ground or floor or other lower level [3], and it occurs due to gravity, when the normal processes to keep a person upright fail [2]. As a matter of fact, there are two conditions that need to be verified before a certain fall occurs. First, the person needs to face an external perturbation, and second, the postural control system, that is responsible for maintaining balance, has to fail in response to the perturbation [7]. In other words, a fall occurs when this system is unable to compensate for the perturbation. In this respect, there are several risk factors that can increase the chance of falling and the occurrence of a perturbation. These factors can be subdivided into two categories [2]:

- **Extrinsic factors:** Extrinsic factors are mostly related to an extrinsic cause and examples are using inadequate footwear, walking in uneven pavements or in slippery surfaces, facing obstacles in the environment and poor lightning.
- **Intrinsic factors:** On the other hand, intrinsic factors (patient-related) include age, history of falls, adverse effects from using medication, mobility impairments or neurological disorders that might cause deficits in gait and/or balance.

These factors can either influence young adults and seniors, but what normally happens in the elderly is that falls result from a multi-factorial problem, derived from interaction between intrinsic and extrinsic factors, and not a contribution from one single factor exclusively. For example, a doorstep might only create problems when step height is diminished as in patients with Parkinson's disease [2].

Knowing that the elderly population fall due to multiple factors, the remaining question is why and how it happens. Falls are common among any age group, but there is a greater incidence and severity in the elderly. However, it is not necessarily a causal relationship, since around 20% of older people still have a completely normal gait and do not fall despite their age [2]. This evidence helped to conclude that

age is not a significant fall risk factor under favorable health conditions, body composition and balance [8]. Moreover, it is not age per se that increases the risk of falling, but instead other comorbidities that emerge with age. In those cases, it becomes necessary to look further to understand what comes from aging that can really affect fall risk.

Muscle weakness is one of the most common intrinsic risk factors that arises with age. As known, muscle strength plays an important role in postural control [9]. This postural control works with the Central Nervous System (CNS) to generate patterns of muscular activity required to regulate the relationship between the body Center of Gravity (CoG) and Base of Support (BoS) [7]. In order to achieve postural equilibrium, it is necessary that the CoG is positioned over the BoS, so that body weight is centered over the feet, as illustrated in Figure 2.1. When the CoG moves outside the BoS provided by the feet against the floor, a fall may occur. Thus, in theory, a weakening of the muscles causes a difficulty in regulating the CoG and BoS interactions, and therefore maintaining balance and avoiding falling. For example, hip movements are important for balance recovery, hence an impairment on the proximal muscles could lead to a potential fall, for lack of reactive balance control. Also, compromises in the joints may increase the risk of falling since they help to maintain upright balance as well [1]. For that reason, remaining active and doing strength exercises can reduce falls by improving global balance [9].

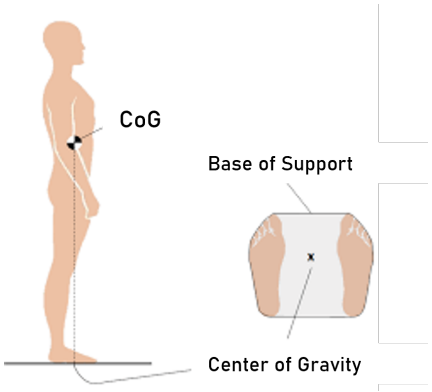

Figure 2.1: Vertical Alignment between center of gravity and base of support [10].

Postural Instabilities have also been identified as one of the main factors that contribute to falling, mostly due to changes in the neural sensory and musculoskeletal systems that can lead to balance deficits [7]. Changes in those systems affect the postural control system and, consequently, the CNS on the stabilizing response to sudden loss of balance.

Pathologies have, as well, been identified as age-related comorbidities, and in most cases can explain gait impairments in elderly people. Diseases like Parkinson's and Huntington's have proven to present changes in gait and an increase in the occurrence of falls [11] [12]. Non-related to pathologies, walking characteristics can also be correlated with increasing age. In general, there is a reduction in walking speed compared with younger people and an increased variability in foot placement during walking [13]. Different circumstances may be responsible for this variability, such as muscle weakness, which has already been discussed as a cause of disturbing stability control. Additionally, aging can lead to motor control impairments that could explain a higher propensity to self-induced perturbations, such as tripping over your own foot, as well cognitive and perceptual deficits which result in a lower capacity of judgement to evaluate, identify and avoid environmental hazards [7].

The most frequent falls in the elderly occur due to postural changes and impairments in gait and/or balance, where in those cases a disturbance in the center of gravity may increase the risk of falling [1]. These falls can be classified into two categories: i) Base of support falls, when the fall is caused by foot

displacement due to a slip, trip or overstepping, and ii) Center of gravity falls related to trunk instability and control when, for example, bending or turning [2]. Regarding the frequency of these falls and the fact that 50% of them occur during walking [7], it is expected that many strategies of evaluating fall risk aim to analyze gait, and, specifically, changes in both foot placement and center of gravity.

2.2 Fall Prevention Strategies

There is an urgent need to develop strategies that help to decrease the number of fall occurrences every year and, at the same time, improve the quality of life of people who have been victims of falls. The financial, physical and emotional costs involved are the principal reasons that motivate new investments of solutions in this research area. Preventive strategies are focused on reducing fall risk factors, such as physical factors, whose influence in falls can be reduced by changes in lifestyle (e.g., exercise). In this respect, exercising and remaining active have proven to be very effective at reducing falls. Beyond physical activity, using walking aids can also be recommended to assist patients with balance problems and to help prevent falls by providing a greater base of support [14].

There are currently two types of systems that aim to solve this major public health problem: i) Fall Detection systems and ii) Fall Prediction systems. These systems can either work with people who have already experienced a fall and with people who have not.

2.2.1 Fall Detection

Fall detection systems are the most common approaches in this topic. This kind of system focuses on detecting a fall in real time by using information either from wearable sensors that can be integrated into watches, shoes or belts or from vision-based systems that can be installed into home environments [4]. One of the purposes of these systems is to reduce the time in which an individual remains involuntarily on the ground after a fall. Therefore, once the fall is detected, these systems typically sent an alert in order to the person receive assistance as soon as possible. This alert can be sent to the caregiver who is expected to take immediate action, and later to the responsible clinician that can improve the medical care provided.

Especially in wearable systems, threshold-based algorithms are often used to detect a fall, by comparing measured values to established thresholds [4]. However, with the breakthrough in machine learning algorithms, methods based on thresholds have become even less preferable.

Fall detection systems basically center on alerting when a fall event occurs, but at the same time can have a direct impact on reducing fear of falling. This fear of falling can be affected by the user perception of the reliability and accuracy of the fall detector, so the higher the accuracy and the faster the assistance provided to the user [15], the higher the chances of reducing this fear.

2.2.2 Fall Prediction

Fall prediction systems can also alert the subjects as the previous system, but the principal difference is that they alert before the occurrence of a possible fall, thus preventing its future consequences, while fall detection systems operate posterior to a fall. Two ways are possible for predicting falls:

- **Fall occurrence prediction**: This approach aims to alert the subjects in real time before a fall occurs by identifying scenarios and circumstances that can lead to a fall. In some of these, people can wear an exoskeleton that is able to detect an occurrence of an external perturbation during

walking, and in order to prevent the person from falling, the device response is to counter react the perturbation and restore subjects' balance [15].

- **Fall risk prediction:** This approach, analogous to the developed in this thesis, aims to alert the subjects of their current risk of falling (none, low or high) by analyzing their gait and/or posture during walking or executing determined task [6]. Through this analysis may result reliable fall risk indicators that can help clinicians to change their current therapeutic strategy and design customized treatment, in order to better prevent falls from happening.

2.3 Gait Concepts

Gait can be defined as a combination of coordinated and cyclic movements that result in human locomotion [16]. For any form of bipedal walking to occur, requisites like periodic leg movement and sufficient ground reaction forces applied through the feet to support the body are importantly necessary [17]. It is the periodicity of each foot moving from one position of support to the next position that makes gait a unique phenomenon.

In the body, there is a sequence of events that must take place so that walking occurs and these events require interactions between the central nervous system, Peripheral Nervous System (PNS) and musculoskeletal system. Understanding this can help to discover possible underlying causes that can affect gait, as well as its further implications. This group of events, which is illustrated in Figure 2.2, can be summarized as follows [17]:

1. Gait command is received and processed by the CNS;
2. Gait signals are transmitted to the PNS;
3. Muscle pattern activities are generated in response to gait signals;
4. Forces are generated at synovial joints;
5. Joint forces are regulated by rigid skeletal segments;
6. Displacement of the segments is recognized as gait, due to muscular activity and joint forces;
7. Ground reaction forces are generated to support the body on the ground;

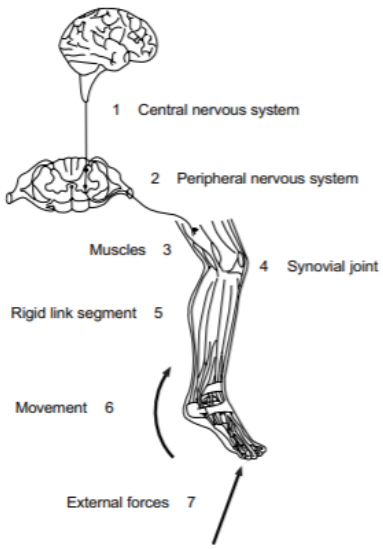

Figure 2.2: Sequence of events behind walking [17].

2.3.1 Gait Cycle

Walking starts as the heel reaches the ground. At the same time, the corresponding limb acts as a source of support on the floor while the opposite limb advances to a new support site, reversing their roles repeatedly over time. This interval of time between any of the repetitive events of walking is called gait cycle and normally is defined as the period between consecutive heel contacts of the same foot with the ground.

A gait cycle can be divided into two main different phases according to the movement of the observed foot: stance and swing phases (see Figure 2.3). The stance phase begins with the initial heel contact on the ground and it refers to the period in which the foot that started the cycle (= observed foot) is in contact with the ground. This phase is equivalent to about 60% of the gait cycle, whereas the remaining 40% correspond to the swing phase, which is the period when the same foot is off the ground [17].

Alternatively, a gait cycle can also be subdivided into double support phase and single support phase, with each occurring twice in one cycle [18]. Considering Figure 2.3, the cycle begins with the initial contact of the observed foot; since at this time the opposite foot is still on the ground, it is a double support phase. As soon as the opposite foot leaves the ground, only the observed foot remains in ground contact in a flat foot position, making this the first single support phase. After the opposite foot reaches the ground again, at the pre-swing phase, there is the second double support phase of the gait cycle. Both double support phases occur during the stance phase. Lastly, the swing phase begins with the observed foot leaving the ground and completing the second single support phase.

By convention, one gait cycle can be characterized by eight sequential events, five during the stance phase and three during the swing phase. These events, depicted in Figure 2.3, can be defined [17]:

1. **Heel strike / Initial contact:** It initiates the gait cycle and it corresponds to the period in which the heel of the observed foot first meets the ground;

2. **Loading response / Foot flat:** It occurs when the observed foot is in complete contact with the ground, while the body weight is transferred onto the forward limb;

3. **Mid-stance:** It is the initial period of single leg support, when the opposite foot is swinging through the observed foot;

4. **Terminal stance / Heel off:** It corresponds to the period in which the heel of the observed foot loses contact with the ground;
5. **Pre-swing:** It is the last event of the stance phase, which begins immediately as the heel of the observed foot lifts the ground, enabling the body weight to move forward.
6. **Toe off / Acceleration:** It starts with the observed foot leaving the ground and with an activation of muscles to accelerate the leg forward;
7. **Mid-swing:** It begins with the observed foot passing directly beneath the body and it is equivalent to the mid-stance for the opposite foot;
8. **Terminal swing / Deceleration:** It corresponds to a slowing down of the observed leg, enabling the stability and position of the observed foot to begin a new gait cycle;

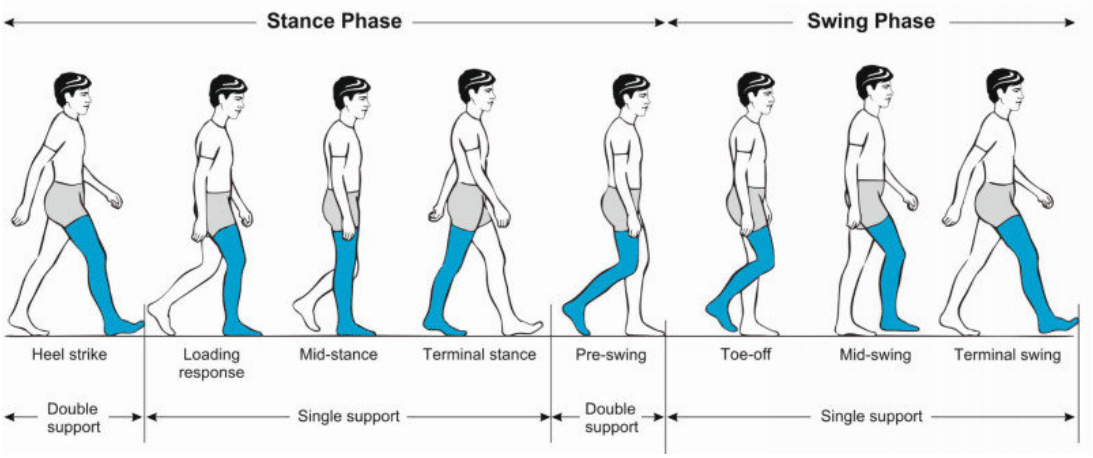

Figure 2.3: Gait cycle events based on the movement of the observed foot represented in blue [19].

2.3.2 Gait Parameters

These gait cycle events can be used to estimate a number of kinematic features that can describe individuals' gait. Kinematic features are normally used to evaluate body motion and its parts, and can be categorized into three groups: spatial, temporal and spatio-temporal parameters [17].

Spatial parameters can describe the foot placement on the ground and include:

- **Stride length:** distance travelled in two consecutive steps and can be measured as the length between two heel strikes.
- **Step length:** distance between a heel contact of one foot and the following heel contact of the opposite foot. For one stride length there is a right and a left step length.
- **Step width:** also known as base of support, is the mediolateral distance between feet, and can work as an indicator of balance problems.
- **Joint angles:** angle measured between two body segments at a given joint, with the most common ones being ankle, hip and knee.
- **Foot angle:** angle between the movement direction and the middle line that passes through the foot (see Figure 2.4).

One stride length makes two step lengths (left and right) as represented in Figure 2.4, but for certain individuals with pathological gaits this measure can be asymmetric when comparing right and left sides.

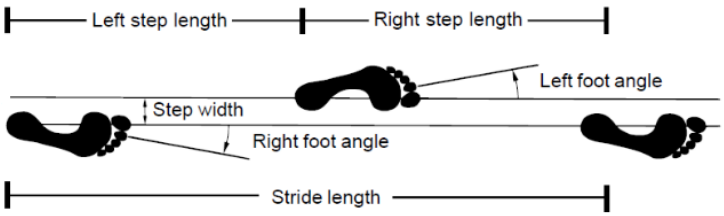

Figure 2.4: Spatial Parameters evaluated during gait [19].

Temporal parameters include time related-features, such as:

- **Stance time:** duration of the stance phase.
- **Swing time:** duration of the swing phase.
- **Double support time:** duration of the double support phase, which is time when both feet are in contact with the ground.
- **Pre-swing time:** duration of the second double support phase that occurs immediately before the swing phase.
- **Single support time:** duration of the single support phase, which is the time when only a single foot is in contact with the ground.
- **Gait cycle time:** duration of the complete gait cycle, which can be estimated as the sum of the stance and swing phase times.

Spatiotemporal parameters include measures from both spatial and temporal domains, such as:

- **Cadence:** average number of steps per minute, within a given period.
- **Speed:** distance covered per unit of time, also known as velocity.

Apart from kinematic features, there are other kind of features that can describe someone's gait and be acquired while walking:

- Kinetic features, describing the forces and moments applied to individuals such as the Ground Reaction Forces (GFR).
- Electrical activity produced by muscles, normally recorded using an electromyography (EMG).
- Body posture and symmetry between each side of the body.

The measurement of these gait features can be accomplished by using different approaches and systems, depending on the type of application. Analyzing and understanding changes over time in all these parameters can help to evaluate human gait whether for the assessment of pathological conditions or for the recognition of a person's walking.

2.4 Gait Acquisition Systems

There are several ways to analyze gait, but considering the number of situations that can be missed by naked eye observation, traditional methods that usually rely on the subjective evaluation of the clinicians are being left behind, being complemented or replaced by a new generation of acquisition systems — Sensor-based and Vision-based [20]. These systems, which can be classified as either vision-based or sensor-based, can be used to capture gait information and provide a more efficient and accurate measurement to clinicians, who can therefore receive more reliable information about a certain individual in a timely manner.

2.4.1 Sensor-based Systems

Sensor-based systems are subdivided into non-wearable and wearable sensors, and each one of them can be easily adapted for clinical diagnosis, treatments, procedures, as well as monitor gait outside clinics [20]. Non-wearable sensors, such as force platforms, are normally found in research facilities, where subjects walk on a marked walkway, with pressure and GRF sensors placed on the platform to capture gait data [21], as illustrated in Figure 2.5a. This platform is able to measure the GRF exerted by the ground on a body in contact with it when walking, as well the center of pressure components.

By contrast, wearable sensors are attached to several parts of the body, such as the feet, knees, thighs or waist, and can be used outside a laboratory to capture gait information during everyday activities. Some examples are Inertial Measurement Units (IMUs) (see Figure 2.5b), force sensitive resistors and EMG systems (see Figure 2.5c). IMUs use a combination of sensors, such as accelerometers, gyroscopes and sometimes magnetometers, that together measure acceleration, velocity and orientation through linear and angular motion. EMG systems detect electrical activity in response to muscle contraction, while force sensing systems normally attached to footwear insole measure GRF under the foot [20].

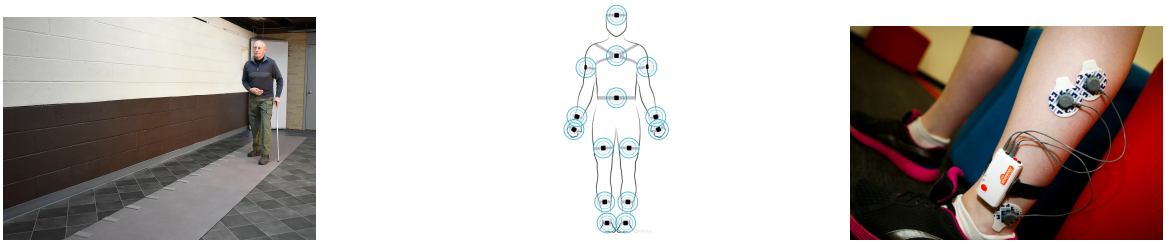

(a) (b) (c)

Figure 2.5: Sensor-based systems. a) Pressure sensitive walkway [22]; b) IMUs [23]; c) EMG system [19].

Most sensor devices are used due to their accessibility in terms of low cost and portability. Such systems can operate during everyday activities, continuously monitoring gait in uncontrolled environments, while giving rich and precise information for real time gait analysis [20]. However, several factors can contribute to displacement of sensors during walking, orientation can be disturbed and errors might happen in measurement of sensor readings [24]. Moreover, these sensors can be very intrusive due to their attachment to rigid segments of the human body, thus causing discomfort at an older age [25], and sometimes they can also be heavy to wear [20] and influence people's gait. For that reason, when working with the elderly, it is important to consider other reliable options.

2.4.2 Vision-based Systems

To address some of the disadvantages mentioned above about sensor-based systems, several methods using a video-camera as an acquisition system and relying on computer vision techniques to analyze the gait were introduced. In the case of vision-based systems, there are also a number of factors that can influence either the captured motion pattern or how the gait is perceived. The motion pattern can be altered by footwear or by the walking surface and the appearance of the subject in the captured footage can be affected by changes in clothing and camera viewpoint. In some cases, subjects tend to cover motion impairments when they know that they are being recorded. Other considerable drawbacks of these systems are related to data privacy and the inability to track persons outside of the camera's range of visibility. Nevertheless, most of these factors can be avoided and overcome, so this is a system that clinicians are interested in for acquiring high quality data [26]. These systems can be classified into either marker-based systems, when using Motion Capture (MOCAP) systems, or markerless systems, when relying only on video-cameras to capture information:

- **Marker-based systems:** Rely on the use of MOCAP systems to record the movement of objects or people. Originally created for gait analysis, these systems are also widely used by sports therapists, neuroscientists, and for validation and control of computer vision systems [27]. This system requires a setup composed of multiple calibrated optical sensors or infrared cameras to capture information with reflective markers attached to different key body positions — see Figure 2.6. Body motion is detected based on the principle that optical sensors or infrared cameras track reflected light by the markers and combine information from multiple cameras to estimate coordinates in three-dimensional (3D) space [24]. Many hospitals and clinics already use systems such as Vicon or Optitrack, due to their high precision and complete trajectory information [28]. MOCAP systems tend to be expensive and demand certain setting and calibration processes, thus can only be used under a controlled environment. By being restricted to laboratory settings, the captured information may not reflect gait in real world situations [20].

(a) (b)

Figure 2.6: Motion Capture (MOCAP) System. a) Setup with cameras installed [29] ; b) Reflective Markers [30].

- **Markerless systems:** Can either use depth-cameras or 2D cameras [31] to acquire data relative to gait. Systems that choose to use depth sensing cameras are capable of reconstructing any scene and estimating body positions in 3D, but in contrast with traditional MOCAP systems, depth cameras do not rely on physical body markers. Instead, they use a pattern of near-infrared light to perceive depth. In other words, it is like a depth camera generating its own body markers made of

light. Figure 2.7 illustrates the composition of a depth camera — Red-Green-Blue (RGB) camera, infrared sensor and infrared emitter.

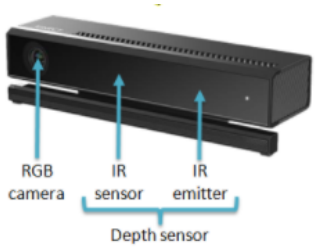

Figure 2.7: Composition of a Depth Camera [32].

Systems that rely on multiple 2D cameras make it possible to capture images from different viewpoints and combine information from each one of them. Yet, markerless systems can acquire data using only a single 2D camera to capture image sequences. Since major articulations during a gait cycle occur in the sagittal plane, using one single 2D camera on a side view observation can be a viable option to perform gait analysis [33]. A downside of choosing this approach is the lack of depth information, limiting its precision. On the other hand, these systems are cheap, accessible, can be implemented under an uncontrolled environment [31] and used during everyday life activities through the video-camera of a smartphone, for example. Additionally, they have an easy installation process without requiring any calibration and are non-intrusive for vulnerable populations, such as the elderly, due to the absence of markers attached to the body. For those reasons, in this thesis, a 2D video-camera was the system chosen to perform gait analysis.

2.5 Gait Analysis System Architecture

Systems proposed to perform 2D video gait analysis are normally composed of three main modules, following a general architecture as the one represented in Figure 2.8:

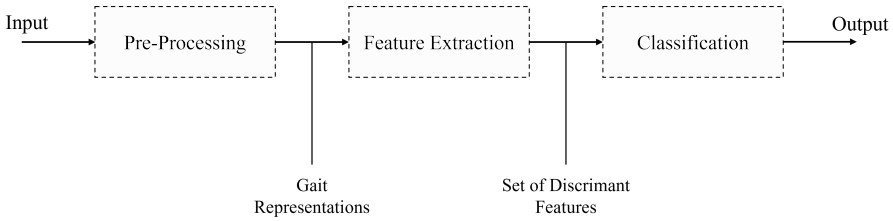

Figure 2.8: System general architecture to perform 2D video gait analysis.

- **Pre-processing:** The purpose of this module is to prepare acquired data to be processed. This includes converting video sequences into valuable gait representations, like human silhouettes or skeletons.
- **Feature extraction:** This module accounts for extracting features that best describe and characterize individuals' gait from the gait representations. In a classification system, the selection of relevant and discriminant information can improve the performance of a classifier.
- **Classification:** This final module receives as input a set of the extracted features and it classifies each observation in its respective class. Examples of the most common classifiers for this purpose

are machine learning algorithms, such as Support Vector Machines (SVM), logistic regression and decision trees.

Chapter 3

State of the Art: Fall Risk Assessment and Gait Analysis

This chapter is focused on providing a literature review on the existing approaches to assess fall risk and on the different methods to perform gait analysis in 2D video data. Section 3.1 reviews the available approaches to assess fall risk in the elderly, from the most traditional to the most recent methods. Section 3.2 includes a brief description of the previously developed methods to pre-process input data using 2D vision-based gait analysis systems, and Section 3.3 enumerates the type of features that can be extracted from that pre-processed data to evaluate fall risk.

3.1 Fall Risk Assessment

Fall risk assessment started to be widely performed with the aim of identifying higher risk individuals among the elderly population and provide them specific interventions. Although fall risk can be assessed through several approaches, there is still no consensus on a methodology that should always be used. The most traditional methods rely on the use of scales and forms to evaluate who is likely to fall based on intrinsic and medical characteristics of the individual. This includes the assessment of psychological status, mobility dysfunction, fall history, acute/chronic illnesses, and sensory deficits [34]. These scales are tools that give a numerical value to various risk factors according to what people answered, with the sum of these factors then used to calculate a final score that predicts if the patient has a low, medium or high risk of falling. The most common scales [35] are the Morse fall scale [36] and STRATIFY [37], which are normally requested by nurses upon admission to a hospital or long term care facility:

- **Morse fall scale:** Tool normally used in acute care settings to assess patient's fall risk upon admission. It consists of six variables (history of falling, secondary diagnosis, ambulatory aid, intravenous therapy/heparin lock, gait and mental status), each one with a score. At the end, the scores corresponding to the six variables are summed to obtain a final score. The final score, which can have a value between 0 and 125, can be interpreted as: no risk (0-20), low risk (25-50) and high risk (>51) [36].
- **STRATIFY scale:** Tool developed to be used to predict falls in the hospitalized elderly. It is based on 5 items (history of falls, patient agitation, vision impairment, incontinence and mobility), where each item has a score of "1", if present, or "0", if absent. The total score is obtained by summing the answers to the five questions, ranging from 0 to 5, and can be interpreted as: low risk (0), moderate risk (1) and high risk (>2) [37].

With information from the scores, clinicians can decide what to do next with patients who have a moderate or a high risk of falling: either assess the patient more frequently or intervene in advance by recommending to do exercise or to use walking devices, with the aim of reducing the risk of falling.

It is also common to assess fall risk through functional tests. This assessment is normally performed by physiotherapists and it is focused on analyzing functional limitations in gait and balance in the elderly community [34]. During these tests, patients can be asked to walk, get up from a chair or to stay balanced for a certain amount of time. The selection of the appropriate test to evaluate a certain patient is still uncertain, although the most widely performed ones are Timed up and Go (TUG) test [38], Berg balance test [39] and Tinetti test [40], each one described as follows:

- **TUG test:** Test to assess patients' mobility, frequently used in the elderly population. The test consists in asking the patient to stand up from a chair, walk for 3 meters, turn 180 degrees, walk back to the chair and sit back down, and it normally takes less than one minute to complete. The time someone takes to complete the test is used as a measure to evaluate fall risk [39], where more than 13.5 seconds corresponds to a higher risk of falling [41].

- **Berg balance test:** Test to assess patients' balance during a series of predetermined tasks, taking approximately 15 minutes to complete. The patient is asked to perform tasks such as sitting, standing and turning, and to repeat it in different conditions — with/without support, with eyes closed/open, with one foot/both feet on the ground. It is a 14-item list, where each item is given a score ranging from 0 to 4, with a "0" score indicating the lowest level of function and a "4" score indicating the highest level. A final score less than 45 indicates individuals who are at a higher risk of falling [39].

- **Tinetti test:** Test to assess balance and gait in elderly people, taking about 20 minutes. It is divided into two sections: the first one assesses balance while siting and standing from a chair, and the second assesses gait on a 15 feet walkway. Both sections are individually evaluated, with gait being scored from 0 to 12 and balance from 0 to 16, corresponding to a maximum total of 28. The lower the score, the higher the risk of falling; a score of less than 18 means the patient is at a higher risk [40].

During these functional tests, subjects are evaluated according to their performance, with fall risk being determined by the observational evaluation of physiotherapists. Normally, they look at subjects' postural stability, gait, and time and difficulty to complete the task. For that reason, this kind of assessment is dependent on the physiotherapist who evaluates, and can also be conditioned by human error, subjectivity and imprecision. Additionally, this type of approach does not acquire intensive and quantitative assessment of the subjects under evaluation, thus more objective methods have started to be included for this purpose. Recently, fall risk have started to be assessed using a combination of traditional approaches (e.g. functional tests) with automatic gait analysis systems (sensor-based or vision-based).

The simplicity and ease in replicating the TUG test, makes it widely used to classify individuals' fall risk. During the test, individuals are asked to perform tasks that are part of everyday life, making an ideal test to identify changes in gait parameters during the performance of the same tasks in other environments. So, several studies were developed with the aim of automatically extracting other parameters during the TUG test besides its duration. Data can be collected using either video-cameras or sensors, which can lead to more information being gathered than when relying only on clinical evaluation. Focusing only on studies using a 2D vision-based system, Skryba et al. [42] used two webcams to extract

body silhouettes and from that automatically compute a number of parameters. Their main conclusion was that the walk duration and the time between turning and sitting back in the chair were the most significant parameters to discriminate between high and low risk individuals. Instead of extracting silhouettes, Lohmann et al. [43], by using a kinect camera, tracked body skeletons. They detected several main events during the TUG test, such as "moving", "start walking", "start rotating", etc, and compared them with events obtained by manual labeling. Other authors chose to analyze a specific component of the test rather than the complete test. Wang et al. [44] used video-cameras to extract body silhouettes. By determining two key parameters, such as "turn time" and "turn steps", their analysis was focused on the turn phase. On the other hand, Frenken et al. [45] analyzed step length and step duration during the walking phase.

Other studies combined both clinical assessment and objective acquisition systems. Romeo et al. [46] assessed balance control in elderly people by performing balance tests to each individual while capturing video information to later extract features.With these exercises they were able to establish the risk of falling for every participant, while at the same time, features relative to body and feet position were extracted. The extracted features were categorized into predefined classes related to the execution of the tests, which implicitly refers to the risk of falling of the patients. They concluded that subjects that revealed an oscillation in the vertical alignment of the body were more susceptible to falling.

It is also common to not rely in any functional tests predefined, and only extract quantitative parameters during gait by using any of the gait analysis systems to assess fall risk. Gervásio et al. [47] aimed to correlate and compare fall risk predictors between group ages using a MOCAP system. They extracted spatiotemporal parameters from gait and their results showed alterations in the parameters, which indicated fall risk between ages of 50 and 70. These alterations included a significant decrease in velocity, stride length and step length, while measures such as stance time, double support time and pre-swing time increased significantly. Automatically predicting risk of falling was completed by Kingetsu et al. [48] while using a 2D vision-based system. They started by extracting features such as walking speed, stride length, toe height when making contact with the ground, and heel height when landing, and after pre-processing it, features were given as input to machine learning algorithms to classify each subject into 4 predefined classes of fall risk — none, low, medium and high risk of falling.

3.2 Gait Analysis: Gait Representations

Gait analysis systems relying on a video-based approach normally go through a process of transforming input data (video) into gait representations that best characterize individuals' gait. This step is necessary in order that gait analysis can be performed, which includes feature extraction and fall risk evaluation, as mentioned in section 2.5. These gait representations can be classified as either appearance-based or model-based, depending on the type of information acquired [49].

3.2.1 Appearance-based

Appearance-based gait representations tend to reflect the shape and/or motion of the moving object, and are typically obtained directly from the frames of a single 2D video sequence. The most common representation is the human body silhouette, which results from performing background subtraction on the original frames. This is an usual step in appearance-based approaches since gait analysis does not normally use the original input, but instead, in this case, removes the background in order to isolate the subject, as demonstrated in Figure 3.1. This pre-processing step is accomplished by using as model a

static background frame and subtracting the other frames containing the moving subject from it. The result of this subtraction is a foreground mask representing the observed subject, which is then converted to a binary output. In order to produce a cleaner binary mask with fewer errors, the obtained mask could also go through a noise reduction process such as filtering.

There are a number of factors that can influence background subtraction, such as the presence of other non-relevant objects in the background, shadows or even variations in lighting. Making sure that light is evenly distributed and does not change significantly during the video sequence is an important step to ensure a good foreground mask is obtained.

(a) (b)

Figure 3.1: Example of background subtraction [50]. a) Original frame; b) Corresponding foreground mask after subtracting the background.

Once the foreground mask is computed, the next stage of gait analysis can be pursued, which is feature extraction. Thuc et al. [31] performed feature extraction from silhouettes to predict fall risk and to detect fall events. For background subtraction, they opted for a Gaussian Mixture Model (GMM) based algorithm to extract the moving human. This approach is based on a probabilistic model that learns which part of the frame (foreground or background) each pixel belongs to. After this learning process, a foreground mask is obtained. The binary silhouette in each frame is then transformed into a reduced representation set of shape based-features to distinguish abnormal from normal gait, as opposed to most approaches that choose to compute biomechanical features that describe gait characteristics. Also to detect abnormal and normal gait, Nguyen et al. [51] extracted motion features from the binary silhouettes, such as motion variation and inclination angle.

An additional gait representation that derive from the human silhouette is, the widely known, Gait Energy Image (GEI). GEI can be computed by averaging every normalized and aligned binary silhouette over one gait cycle, as in equation 3.1:

$$GEI(x,y) = \frac{1}{N}\sum_{i=1}^{N} B_i(x,y) \tag{3.1}$$

where N is the number of frames contained in a gait cycle, and B_i (x,y) is an aligned binary silhouette image at frame i, with x and y as its pixel coordinates.

The resulting GEI is a gray-level image that provides robustness to variation and can deal with missing parts of a given silhouette derived from background subtraction. This happens because GEI considers all the silhouettes within a gait cycle, which means that missing parts from one silhouette can be complemented by other silhouettes and minimized in the final image, as represented in Figure 3.2. As a whole, it reflects major shapes of silhouettes and highlights changes over the gait cycle, such as the movement of the limbs.

Figure 3.2: Example of GEI robustness in the presence of shadows in the corresponding silhouettes [52].

Ortells et al. [26] performed feature extraction using gait representations with the aim of quantifying gait impairments and relate them to increased fall risk. Features such as intensity (amount of movement), amplitude (limb's movement broadness) and gait asymmetry were calculated from the GEI, while stance phase duration, swing phase duration, step length, as well as asymmetry, were computed using the binary silhouettes. Also, in [53] gait features were estimated using both silhouettes and GEI. In this study, features were divided into: i) Feet-related, when using silhouettes to extract spatio-temporal information from feet displacement over a gait cycle, such as step length and speed, and ii) Body-related, when using GEIs to extract body information derived from the individuals' posture, such as amount of movement, a shift in center of gravity and torso orientation. Those features, besides being extracted to classify gait impairments, were mentioned as possible indicators to determine fall risk.

3.2.2 Model-based

Model-based gait representations aim to fit a model to the moving object, whether a structural model or a motion model. Structural models are models that describe the shapes of each part of the human body, such as head, torso, hip, thigh, knee and ankle, while motion models describe the kinematics and motion dynamics of those body parts [49].

Typically, to fit a structural model to a moving body, human body part positions are tracked and tagged with key-points. The connection of those key-points with line segments results in a human skeleton, as the one depicted in Figure 3.3a. In addition to this example, the model can be composed of other arbitrary shapes representing the edges of body parts, such as ellipses, cylinders or cones, as shown in Figure 3.3b.

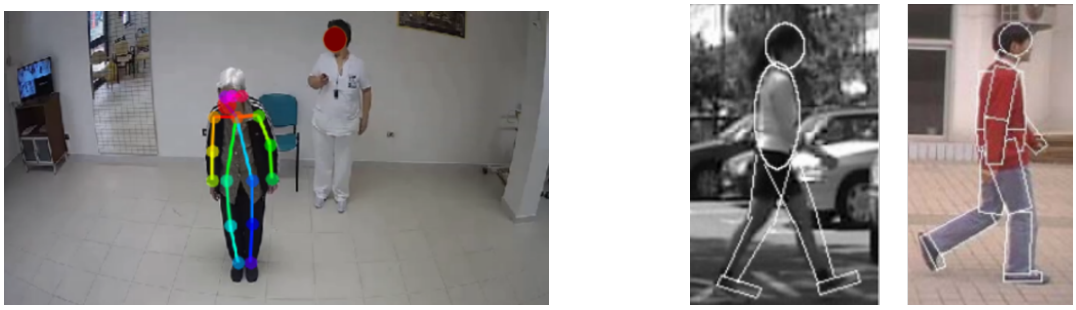

(a) (b)

Figure 3.3: Example of structural models. a) Skeleton tracking using body key-points [46] ; b) Other arbitrary shapes to represent the body parts [54] [55];

From these representations, spatiotemporal features, such as speed and step length, as well joint angles and joint distances, can be extracted by using the key-points as references. To detect the human skeleton, Romeo et al. [46] used the OpenPose library [56], a pre-trained deep learning-based human pose estimation model. It enabled the identification of 18 skeleton joints and, once identified, the software connects them into a skeleton, tracking their real time position in every frame, as represented in

Figure 3.4a. Knowing the positions of each joint in every frame, the authors of [46] computed the distance between feet, distance between hand and hip, and body posture. Then, they fed those features into a decision tree classifier to predict fall risk. As mentioned earlier in this chapter, this study combined clinical evaluation with quantitative feature extraction, achieving a final risk prediction of 79.1%. Kingetsu et al. [48] also used OpenPose to extract human skeletons. The spatial coordinates obtained from the key-points of the skeleton allowed them to estimate stride length, walking speed and toe and heel height. With these features, a SVM classifier obtained 100% of accuracy in the fall risk classification.

Rather than using only skeletons and their key-points positions, similarly to GEI, a gait energy image using skeletons can be computed as done by [57], in the scope of abnormal gait classification. With the binary human skeletons of one gait cycle, an average skeleton image can be obtained using the same method of GEI, represented in Figure 3.4b.

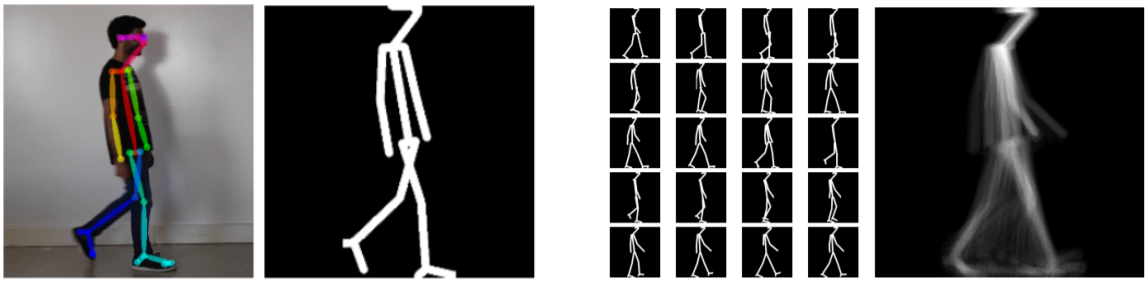

(a) (b)

Figure 3.4: Skeleton Gait Energy Image (SGEI) Computation [57]. a) OpenPose output and corresponding binary skeleton; b) Human skeletons during a gait cycle and the final SGEI.

Concerning motion models, the type of features that can be extracted results from modeling human gait with the change of key-points positions over time. Common features include angular measurements or movement trajectories, computed by determining body parts positions in every frame and tracking them across the entire video sequence. In [58], they obtained a structural model using OpenPose, with 13 key-points. Although a human skeleton was used as input, they extracted motion parameters, such as the trajectory of the ankle positions and the center of mass, as illustrated in Figure 3.5. Besides, temporal gait variables such as cadence and step time, as well as distance measures such as symmetry of step width were measured. A statistically significant association was found between these gait features, the clinical assessment performed using Tinetti scale and the number of falls experienced.

Figure 3.5: Motion parameters obtained by tracking ankle and center of mass positions over the video sequence [58].

Model-based gait representations can give information from both human body dynamics and shapes, depending on the type of model that is fitted. The main advantages of these representations are robustness

to self-occlusion and to background noise, contrary to appearance-based approaches where removing the background can be a major difficulty. These models can be either two or three-dimensional, although the most common solution is to extract 2D models due to the high computational cost of fitting a 3D model to a human body. Skeleton tracking systems based on 2D cameras normally rely on open source software to track skeletons, such as the OpenPose library, while to obtain a 3D skeleton, depth cameras are preferred for more robust real-time results.

Using depth cameras allows for a skeleton tracking system to be more robust to different lighting conditions than a single 2D camera. However, the main disadvantages of relying on depth cameras are the difficulty in replicating the setup in unconstrained environments, requiring a calibration step before acquisitions and a limited range of operation, along with the fact of being computational expensive.

3.3 Gait Analysis: Fall Risk Features

There are several gait parameters that can be measured when using 2D gait representations. Some have already been discussed in Section 2.3.2, such as parameters that can be extracted from the gait cycle during walking. These parameters are mainly associated with duration of phases (stance time, swing time, pre-swing time, double support time), distances calculated from the foot placement on the ground (stride length, step length, step width) or even both spatio and temporal domains (velocity and cadence). In gait analysis, all those parameters are classified as spatial-temporal, and are the most common to be extracted and analyzed when using a 2D vision-based system. Fall risk indicators can be defined as any kind of parameters that can indicate that someone is at increased risk of falling. They can be either computed during gait analysis or acknowledged from individuals' information. Among seniors over 65 years old, the most frequent features computed are velocity, step length, stride length, pre-swing and double support time [47]. There is evidence that elderly people present a decreased velocity, step length and stride length, but on the other hand have increased double support time and pre-swing time [47]. As mentioned before, this could be a result of the deterioration of muscle strength with advancing age, leading the elderly population to demonstrate slower gait velocity, reduced step length and loss of stability.

Loss of muscle strength can also cause asymmetrical leg strength, resulting in an asymmetry between right and left sides of the body. Actually, older women with or without a history of falls exhibited asymmetrical leg muscle strength and power, but the fallers consistently showed a significantly greater asymmetry. In order to evaluate fall risk, spatiotemporal parameters of right and left sides can be computed with the expectancy of finding significant differences between them [26] [47]. In addition, people who are at a higher risk of falling present an increased variability in gait due to fluctuations in walking, also related to age. In this sense, it is common to evaluate gait variability in several parameters (stride length, step length) as a measure of fall risk [59] [11] [12].

Loss of balance and instability are the most common causes of fall along with alterations in gait. So, analyzing changes in stability and postural control can work as a fall risk predictor. This analysis can be reflected in evaluating the center of gravity, due to its important role of maintaining balance.

These types of fall risk features can be obtained by analyzing gait during a normal walk, but in addition to it, fall risk can as well be evaluated by estimating gait parameters during the execution of predetermined tasks like the TUG test. Example of gait parameters that can be estimated during a TUG test are speed, step length, number of steps, time to complete the test, time to turn around or time to move from a sit to a stand position.

Apart from that, increasing age and history of falls are information that can also be acquired to help predict an increased risk of falling.

Chapter 4

Materials and Methods

In this chapter, the primary methods applied in this thesis are detailed, as well as the material used for their development. Section 4.1 describes how video data was acquired with the two groups of participants — yound adults and elderly individuals — with a brief description of the experiments, the acquired data set and the participants included in this study. Section 4.2 describes the fall risk evaluation performed by the physiotherapists during acquisitions with the elderly group. Section 4.3 describes the methods used to pre-process the acquired video data and obtain gait representations such as binary silhouettes, 2D skeletons and SGEI. Section 4.4 explains how fall risk indicators were estimated from these gait representations. Finally, Section 4.5 reports the validation process done with *Contemplas* gait analysis software.

4.1 Data Collection

Data collection consisted of acquiring two types of data. The first type corresponded to recording the movement of the participants with a video-camera while the subjects performed some predefined tasks; the second type corresponded to personal data obtained through a questionnaire and it included information such as age, sex, height, weight, history of falls, presence of motor incapacity diseases and use of any kind of walking devices. Although the last four questions were formulated with the elderly population in mind, the same information was asked to both groups of participants as a matter of comparison, as exemplified in Appendix A.

Data was collected in two separate phases, each one with a different group of participants. The first data collection took place at Escola Superior de Saúde da Cruz Vermelha Portuguesa de Lisboa (ESSCVP) and was completed within three full days between late june and early july of 2021. The recruited participants were a group of young adult students, that integrated the control group for this experiment. The second phase occurred in mid october of 2021 and was dedicated to collecting data with the elderly. To avoid their displacement to the ESSCVP, the acquisitions happened at the day care centers they attended.

The same setup was used in both phases of acquisition. It consisted of a Garmin Virb Ultra 30 video-camera, positioned perpendicularly to the direction of movement, in order to record the side view of participants' gait. The video-camera was supported by a tripod and it was placed approximately 3 meters away from the target and at 1 meter from the ground. Video was recorded with a resolution of 1080p at 50 frames per second (fps).

4.1.1 Participants

Thirty-three participants (25 females, 8 males) were included in this study, with ages between 20 and 87 years old (mean = 47.8). They were divided into two distinct groups, one control group composed of 27 young subjects aged between 20-28 (mean = 22.11), and an elderly group composed of 6 senior subjects aged between 59-87 (mean = 73.5). The control group participants were all physiotherapy students attending ESSCVP, while the elderly were part of day-care centers located near the school that receives clinical support at their facilities. The main inclusion criterion was being able to walk at least 6 m straight without any walking device and without assistance. All participants signed a written informed consent form prior to inclusion, available at Appendix C, and the study was approved by the ethics committee of the Faculdade de Ciências da Universidade de Lisboa.

Table 4.1 shows the demographic information inquired with the questionnaire (mean $\pm$ standard deviation) of the two separate groups (control and elderly) who participated in this study. Information regarding fall risk – history of falls, presence of motor diseases and use of walking aid – can be found in Appendix B, as well as the demographic answers to the questionnaire for each subject.

	Control Group ($mean \pm std$)	**Elderly Group** ($mean \pm std$)
Age (years)	22.1 ± 1.6	72.3 ± 9.1
Weight (kg)	67.9 ± 12.9	75.1 ± 11.6
Height (cm)	168.7 ± 8.4	159.9 ± 7.6
Body Mass Index (kg/m^2)	23.8 ± 3.4	29.7 ± 4.8
Female, n	19 out of 27	6 out of 6

Table 4.1: Demographic information of the two groups of participants included in this study.

4.1.2 Experiments description

Data collection consisted in recording participants' gait during two types of activities: i) TUG test and ii) Walking straight for 6 meters. The setup of the TUG test was composed of a 40 cm high armless chair, a tape mark placed on the ground and a video-camera to record the activity. As demonstrated in Figure 4.1, the tape marked a distance of 3 meters from the chair, and it served as an indication of the place where the participants had to turn around. The test begun with participants seated on the chair and, after the physiotherapist's command, the participant had to get up from the chair, walk towards the mark on the ground, turn around after passing it with both feet, walk back to the chair and finally sit back on it. Before the execution of the test, each step was explained to the participants, giving them an opportunity to try it before recording. Video capture started once participants were asked to start the test, with their full-body movement being recorded. Each participant performed the TUG test three times, with a 2-minute break between each run. For the walking activity, the chair was removed from the setup and participants had to walk straight for 6 meters, from the right side of the acquisition lab to the left side and then repeat it in the opposite direction (left to right). This walking activity was completed twice for each participant, thus recording a total of two videos with sequences from both sides. Just like the previous activity, participants had also a 2-minute break between repetitions. In both activities, participants were asked to walk at their normal and comfortable pace.

Figure 4.1: Acquisition setup at ESSCVP, with a standard chair and a white tape positioned on the ground for the execution of the TUG test. For recording the walking activity, the chair was removed from the setup.

Due to the COVID-19 pandemic, participants used a face mask during the entire time of the acquisitions, with the advantage of also safeguarding their identity.

4.2 Clinical Fall Risk Assessment

During the second phase of data acquisition, fall risk was assessed in the elderly group included in this study. This assessment occurred after having the informed consent of the participants and before proceeding with the recordings. Each elderly participant was evaluated using a traditional method of clinical assessment by a group of physiotherapists that attended ESSCVP. Fall risk evaluation was binary, meaning that subjects were only evaluated as either having or not having a risk of falling.

As mentioned early in Chapter 3, there is a variety of options to perform this checkup and, in this case, it was achieved with a tool named self-rated Fall Risk Questionnaire (FRQ) [60]. Table 4.2 includes the type of information that the elderly population was asked in the 13-item questionnaire, whose answers were then used to assess their risk of falling. A FRQ total score can be obtained by summing the total number of points for all "yes" responses, where affirmative answers to questions 1 or 5 give 2 points and to all other questions give 1 point. A total score ≥ 4 indicates that the subject under evaluation has fall risk.

Fall Risk Questionnaire Items	
1. I have fallen in the last 6 months.	yes/no
2. I am worried about falling.	yes/no
3. Sometimes, I feel unsteady when I am walking.	yes/no
4. I steady myself by holding onto furniture when walking at home.	yes/no
5. I use or have been advised to use a cane or walker to get around safely.	yes/no
6. I need to push with my hands to stand up from a chair.	yes/no
7. I have some trouble stepping up onto a carb.	yes/no
8. I often have to rush to the toilet.	yes/no
9. I have lost some feeling in my feet.	yes/no
10. I take medicine that sometimes makes me feel light-headed or more tired than usual.	yes/no
11. I take medicine to help me sleep or improve my mood.	yes/no
12. I often feel sad or depressed.	yes/no
13. Because I don't see well, I have difficulty avoiding hazards in my path, such as tree roots or electrical cords.	yes/no

Table 4.2: Tool used by the physiotherapists to assess fall risk in the elderly group, named self-rated Fall Risk Questionnaire (FRQ). A total score ≥ 4 indicates evidence of risk of falling.

The presented questionnaire worked as a screening tool for the elderly group included in this study and the outcome was that all senior participants revealed evidence of fall risk. Apart from this assessment, within the elderly group, it was observed by the physiotherapists that certain subjects reported major alterations in their motor capability, when compared to the other subjects being evaluated that presented a more standard gait for their age. Although no formal evaluation was performed to determine if the fall risk was high or low, in order to check if the developed algorithm was sensitive to these motor alterations visually identified, this information was registered. From the total of six elderly evaluated, two were reported as having major visible alterations in their gait. For a matter of identification, this sub-group, composed of 2 subjects, can be entitled as Elderly with major gait alterations, and the remaining sub-group, composed of 4 subjects, can be entitled as Elderly with minor gait alterations.

4.3 Data Pre-Processing

4.3.1 Data Organization

Before pre-processing data, each video collected during the walking activity was divided into two. In the recording sessions, subjects walked from one side of the lab to the other and then back in the opposite way. Therefore, the video was divided between sides, which resulted in a total of four different video sequences for every subject (i.e., two for every video recorded). Data was then ready to be organized per subject:

- 3 videos of TUG test;
- 4 videos of walking sequences;
- 1 questionnaire with personal information;

Since the video records of the walking sequences contained more than three complete gait cycles, it was possible to discard some cycles that do not completely reflect subjects' gait and still have left enough gait cycles to analyze. As a consequence, the first and last gait cycles in video records were excluded from the analysis. The first one was discarded based on the evidence that normally it takes at least one or two steps for subjects to walk at their normal pace and the last one because most subjects reduced their step sizes due to approximation to the wall. Therefore, it was decided together with the physiotherapist to not consider these two gait cycles, which in this way could result in a more accurate gait analysis.

4.3.2 Silhouette Extraction

At an early stage of this work, binary silhouettes were extracted using a background subtraction method, since the idea was to have two types of gait representations (i.e., silhouettes and skeletons) extracted from the video sequences.

To obtain a binary silhouette, the first step is to track the human body, or foreground object, present in a video sequence taken with a camera. Each image in the video sequence can be divided into foreground and background, with foreground, in this case, being the target for analysis, and anything other than the human body being classified as background. One of the most common ways to highlight and to segment a foreground object is to subtract the background from the original image.

The background subtraction performed was based on a probabilistic method, involving gaussian mixture models. This method, currently available in the computer vision toolbox of MATLAB [1], works by modelling the value of each pixel as a mixture of gaussian distributions to build a background model. To be applied, it requires the previous definition of four parameters:

- α: this parameter, also known as learning rate for adapting model parameters, controls how quickly the model adapts to changing conditions;
- **Threshold**: The threshold, or minimum background ratio, is used to establish which pixels should be considered for the background model;
- **Number of training frames**: This parameter represents the number of initial frames of the video sequence to be used for training the background model;
- **Number of gaussians**: This parameter represents the number of gaussian modes in the mixture model, normally set to 3, 4 or 5;

To determine which pixels correspond to background, the method looks at the variance of the gaussians on the mixture. Gaussians with a smaller variance are more prone to belong to the background, while gaussians with a higher variance to the foreground. This is explained by the fact that background objects are considered static and persistent over time, thus maintaining a lower variance, in opposition to foreground objects. After foreground pixels are identified, a foreground mask representing the silhouette extracted from the original frame can be defined.

Morphological operations such as *open* —- *erosion* followed by *dilation* — were applied on the binary silhouette to remove pixels outside of the silhouette area. The selected structuring element was squared-shaped with a size of 5×5 pixels, where pixels with a radius less than 5 were removed.

[1] https://www.mathworks.com/help/vision/ref/vision.foregrounddetector-system-object.html

Before data was collected, this method was applied to a test dataset, created in the scope of gait analysis, provided by a former Master student [2]. Results from performing background subtraction to that dataset are illustrated in Figure 4.2.

(a) (b) (c)

Figure 4.2: Background subtraction results on the test dataset. a) Background frame; b) Original frame; c) Binary silhouette after performing background subtraction and applying morphological operations.

Later, this method was applied to a preliminary dataset acquired at ESSCVP, but the final result was far from what was desired. Different setups were built so that background subtraction could be accurately performed, but none of them led to positive results. The main issues were brightness fluctuation over time, presence of shadows and absence of a homogeneous background.

The first tested setup is represented in Figure 4.3a, as well as the obtained silhouettes illustrating the main issues found when subtracting the background.

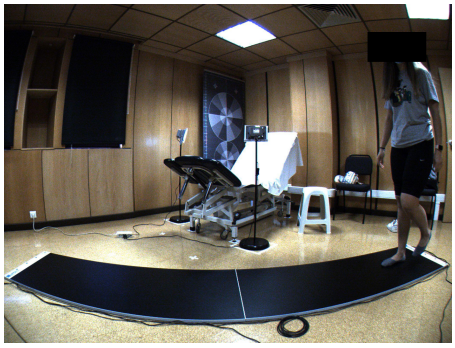

(a)

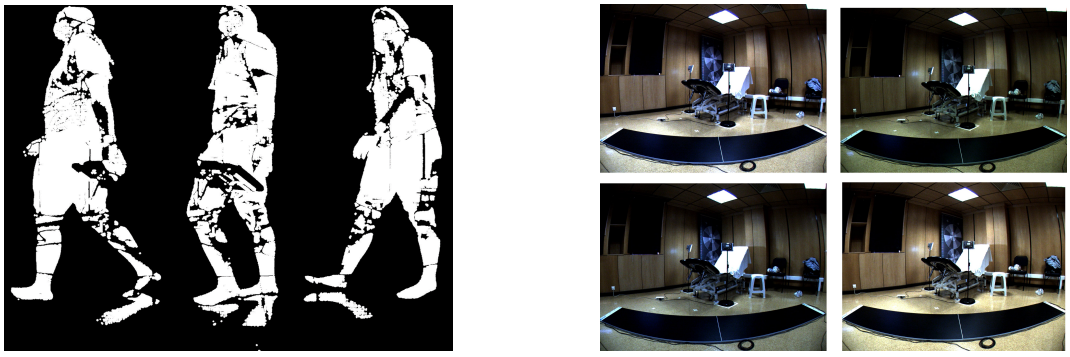

(b) (c)

Figure 4.3: Background subtraction results on the first setup. a) Setup; b) Obtained silhouettes illustrating the main issues of background subtraction c) Brightness fluctuations over time;

Despite the various removable objects that were part of the setup, the subtraction of background was really challenging. One of the main difficulties was the brightness change along the video sequence, as represented in Figure 4.3c. These variations in intensity over time made pixels previously considered as

[2]https://fenix.tecnico.ulisboa.pt/cursos/meec/dissertacao/1128253548922197

background being then wrongly identified as foreground. Also, the way the setup was built allowed the appearance of shadows on the gait platform, illustrated in Figure 4.3b. When the goal is to perform gait analysis, it is also important to avoid having a heterogeneous background and subjects wearing clothes with the same colour as the background since it results in background subtraction errors, as depicted in the middle frame of Figure 4.3b.

Due to the unsatisfying results concerning binary silhouette extraction, the setup was changed, as illustrated in Figure 4.4a. The setup was changed by adding some complements to avoid some of the discussed issues, such as covering with a cloth both the back wall, to attenuate brightness fluctuations, and the ground, to reduce the effect of shadows.

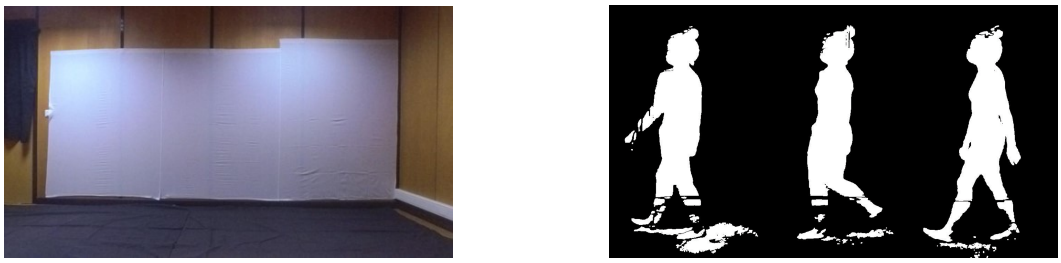

(a) (b)

Figure 4.4: Background subtraction results on the second setup. a) Setup; b) Main errors of background subtraction;

Even though changes were completed on the setup, some of the errors previously mentioned persisted, especially in the feet area, which is very important for the estimation of gait parameters. For that reason, along with the fact that the length of this setup was too short to perform the TUG test (at least 3.5 meters), data collection was not conducted with this setup and only 2D skeletons were extracted from the video sequences.

4.3.3 Skeleton Extraction

Another possible approach to track a human body in a video sequence is human pose estimation. This approach allows to detect several anatomical key-points from body, foot, hand and face, and when linked, skeletons can be extracted as a whole from a single image. To obtain 2D skeletons, the OpenPose software [61] was used, which is known as the first open-source library for real-time pose detection. This system is composed of a convolutional neural network, with two branches that predict two different outputs. The first branch predicts confidence maps of different body parts locations, and the second predicts party affinity fields, which consists of a set of vector fields encoding the location and orientation of limbs over the image. The two output will then be parsed to obtain 2D key-points.

Giving as input a video sequence, the most complete OpenPose body output was selected, BODY25 format, containing a total of 25 key-points, as illustrated in Figure 4.5, with the corresponding labels represented in Table 4.3.

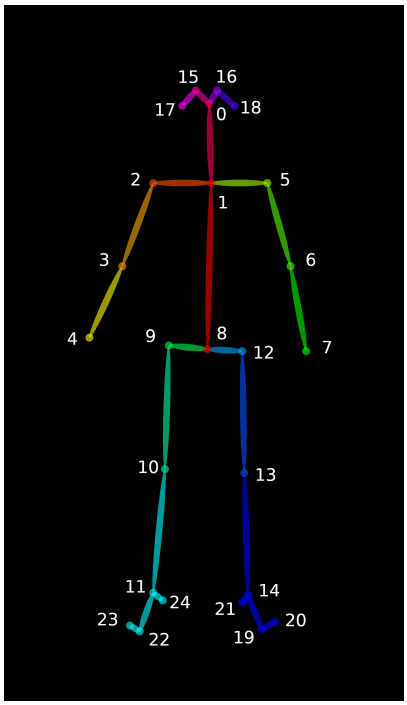

Figure 4.5: OpenPose output: BODY 25 Model [56].

0 - Nose	1 - Neck	2 - Right Shoulder	3 - Right Elbow	4 - Right Wrist
5 - Left Shoulder	6 - Left Elbow	7 - Left Wrist	8 - Mid Hip	9 - Right Hip
10 - Right Knee	11 - Right Ankle	12 - Left Hip	13 - Left Knee	14 - Left Ankle
15 - Right Eye	16 - Left Eye	17 - Right Ear	18 - Left Ear	19 - Left Big Toe
20 - Left Small Toe	21 - Left Heel	22 - Right Big Toe	23 - Right Heel	24 - Right Heel

Table 4.3: OpenPose output key-point labels.

To extract the skeletons, the OpenPose software was run using the Windows Command-line tool [56], which returned as output a video sequence with only 2D skeletons, representing the moving body on each frame of the video, such as the one depicted in Figure 4.5. Optionally, OpenPose can be opened in Python or C++.

When using OpenPose, there are no concerns with background removal, so the next and last step was to convert each frame of the video (i.e., 2D skeletons images) into binary images on MATLAB, using Otsu's Method [62]. This method determines a threshold value that maximizes the separability between the gray levels of the two classes — foreground (i.e., skeleton) and background.

4.3.4 SGEIs Computation

To acquire information from the entire body during a gait cycle, an additional gait representation over time, SGEI, was computed using the extracted binary skeletons. As mentioned early in Chapter 3, SGEI is analogous to GEI, whose only difference is using binary skeletons images instead of silhouettes for computation. For this purpose, a preliminary procedure was completed [52], illustrated in Figure 4.6. This included normalizing each skeleton with respect to their size and aligning them horizontally. The first step was to crop each skeleton according to the dimensions of a bounding box containing only the skeleton region, so that the cropped image has the same size as the bounding box, as demonstrated in Figure 4.6b. The cropped skeletons were then resized to a dimension of 530×530 pixels, to guarantee

that all skeletons had the same height. The next step was to horizontally align the images, and to achieve this, each resized skeleton was centered in respect to the x coordinate of the centroid. By selecting the upper body part of the skeleton, which is equivalent to the first half (=50%) of the image, the centroid was calculated as the center of gravity of this region. The resulting image is illustrated at Figure 4.6c.

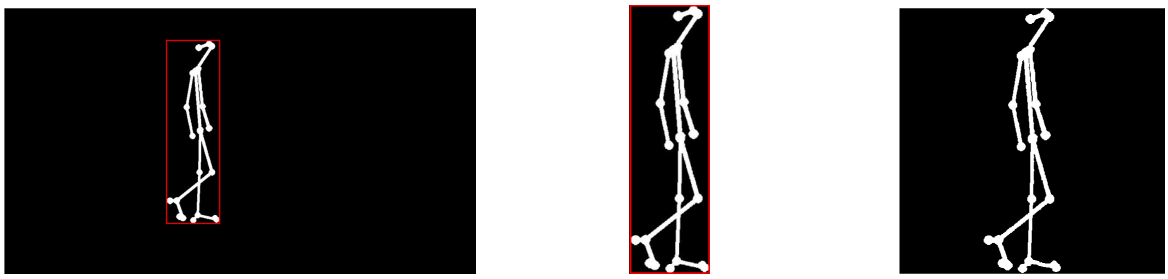

(a) (b) (c)

Figure 4.6: Example of the preliminary procedure performed to the binary skeletons before computing the SGEI. a) Original image with red bounding box containing the skeleton region; b) Skeleton image cropped in respect to its bounding box; c) Final image after being horizontally aligned, with a dimension of 530×530 pixels.

After this preliminary step, a SGEI was computed for every gait cycle of a video sequence, according to the following definition:

$$SGEI(x,y) = \frac{1}{N}\sum_{t=1}^{N} I_t(x,y) \tag{4.1}$$

where N is the total number of frames in a gait cycle, t is the index corresponding to the frame number in the sequence, I is a skeleton image at frame t, and x and y are the image coordinates — see Figure 4.7.

Figure 4.7: SGEI computation for one gait cycle of a video sequence.

According to equation 4.1, a SGEI was obtained by averaging every binary skeleton of a gait cycle, where the resultant SGEI is a gray-level image. A gait cycle can be defined as the duration of three consecutive initial contacts (IC), i.e heel strikes (HS), where the last initial contact of a gait cycle corresponds to the first of the next gait cycle. Therefore, the number of frames, N, was selected by determining the moments in which IC happened during a sequence. Approximately, at an initial contact, the distance between feet is maximum, so in order to determine which frames corresponded to this moment, the distance between feet was computed in each frame by selecting the bottom 10% of the skeleton image, as shown in the Figure 4.8.

Figure 4.8: Bottom 10% of the skeleton image representing initial contact (i.e. heel strike) moment.

If considering a video sequence as the one represented in Figure 4.9a, it can be divided into two gait

cycles, each one containing three moments of IC — the first at the beginning of the cycle, the second between gait phases and the last when the feet return to the starting position, ready to start a new cycle. Still considering this video sequence, two SGEIs were computed, exemplified in Figure 4.9b, one per cycle, where N was calculated as the frames difference between IC_i and IC_{i+2}.

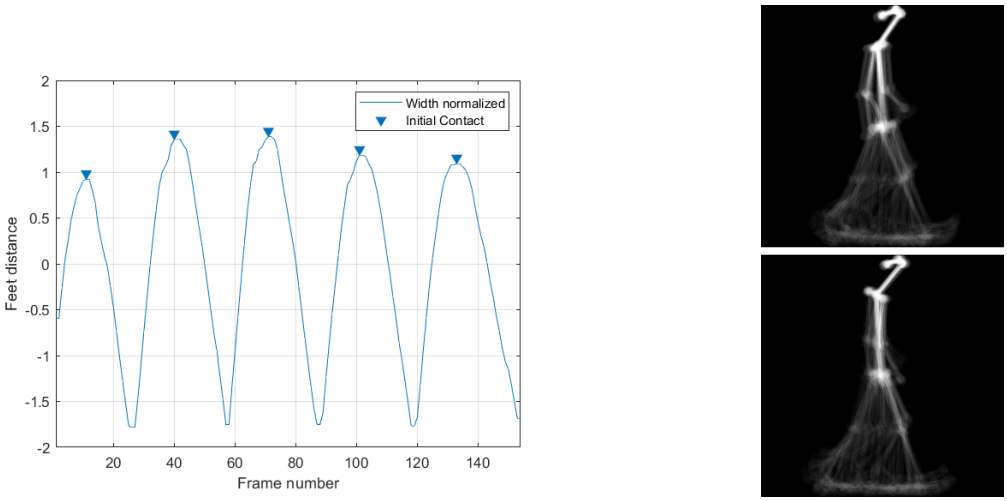

(a) (b)

Figure 4.9: SGEI computation for a video sequence. a) Distance between feet over a video sequence, where maximum distance is represented with the blue markers; b) SGEIs computed for this video sequence composed of two gait cycles.

4.4 Gait Features Extraction

After pre-processing all video sequences, data was ready to be analyzed and consisted of extracting gait and temporal parameters from 2D skeletons and SGEIs.

4.4.1 Walking Sequences Features

Using silhouettes obtained from the lateral viewpoint to extract "hand-crafted" bio-mechanical features to analyze individuals' gait was something that started to be developed by Tanmay Verlerkar, a former PhD student, with the main objective of classifying different pathological gaits [53].

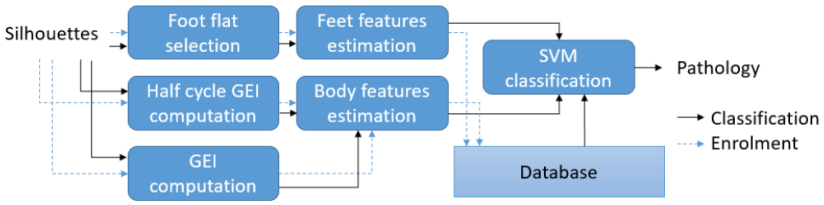

Figure 4.10: Proposed system to estimate bio-mechanical features from binary silhouettes to classify gait pathologies [53].

Part of his proposed system, represented in Figure 4.10, was adapted for this thesis project since some of the features he estimated — step length, speed, shift of CoG, and torso orientation — could as well be computed from 2D skeletons to evaluate fall risk. However, other relevant fall risk indicators not considered in his study were also included here. In this regard, there were two sets of gait features that were computed:

- **Feet-related features:** These features correspond to spatiotemporal parameters that can be extracted by analyzing feet displacement over a gait cycle and can be sub-divided into spatial (distance), temporal (periods), and spatio-temporal parameters, as such:
  - Spatial parameters include step length, stride length, step length symmetry, stride length symmetry and coefficient of variation for stride length.
  - Temporal parameters include stance time, double support time, pre-swing time, and gait cycle time.
  - Spatio-temporal parameters include speed.
- **Body-related features:** These features reflect body positioning during a gait cycle, such as shift of the center of gravity and torso orientation.

Most of these parameters, especially temporal ones, are calculated for each gait cycle at a time and, therefore, the number of gait cycles present in each video sequence must first be detected. This was achieved by looking for initial contacts over the entire sequence, having in mind that one gait cycle contains three consecutive initial contacts.

As explained in Section 4.3.4, initial contacts are detected when the maximum distance between the two feet is reached when walking. To calculate this distance, the feet region from each frame was selected with a bounding box, which corresponds approximately to the bottom 10% of the skeleton, as demonstrated in Figure 4.11. The distance between the feet over a gait cycle was calculated as the width of the bounding box containing both feet, whose width was normalized by subtracting each width value by the mean and dividing it by the standard deviation.

Figure 4.11: Bounding box containing feet region.

Knowing the frame where each IC occurs, gait cycles can be then separately analyzed. Exemplifying, the first cycle will contain frames from IC_i to the IC_{i+2}, the second from IC_{i+2} to IC_{i+4}, and so on until the last IC of the sequence is reached, with i representing the indices of IC during a video sequence. To estimate feet-related features, all flat foot occurrences that happened during a gait cycle were determined. A flat foot (FF) event can be defined as the moment when a given foot is in full contact with the ground during each phase of the gait cycle. So, two flat foot events are registered per cycle, one for each gait phase, i.e. one for each foot. To detect a flat foot event, a Gait Texture Image (GTI) was computed, which is a representation of individuals' walking positions over time. Only the feet region of skeleton images was considered for this computation, in order to avoid the selection of other body parts that are not relevant for this purpose. A GTI was obtained for every half gait cycle by averaging every binary skeleton contained in this interval, using a similar formula as the one used for GEI — see equation 4.2. The main difference is that here the spatial positions of the initial skeletons were maintained (i.e., skeleton images were not aligned), since the objective was to analyze the feet evolution over time. In GEI, the skeleton images needed to be aligned and had all the same size.

$$GTI(x,y) = \frac{1}{N}\sum_{t=1}^{N} I_t(x,y,t) \tag{4.2}$$

where N is the total number of frames in a half gait cycle, t is the index corresponding to the frame number in the sequence, I is a skeleton image at frame t and x and y are the images coordinates.

By selecting all frames contained in a half gait cycle, a GTI was computed with the purpose of highlighting the flat foot positions over time — Figure 4.12a. This was possible due to the overlap among skeleton frames when computing the GTI, with the feet positions with highest overlap corresponding to flat foot positions. This happens because when a foot is flat on the ground, it remains static along a gait phase and during several consecutive frames, thus leading to a high amount of overlap in the GTI. In order to detect flat feet, the Otsu's Method [62] was then applied to the obtained GTI to determine a threshold that maximizes inter-class variance in gray levels. Hence, regions with gray level values above the obtained threshold, were considered to be overlap regions (i.e., flat foot), and were, therefore, selected. So, for each half cycle, the computation of GTI resulted in a new flat foot. Figure 4.12b illustrates all flat foot events detected for a certain walking sequence. Also, after applying Otsu's threshold, FF positions were determined by calculating the centroid positions from each foot, as demonstrated in Figure 4.12c.

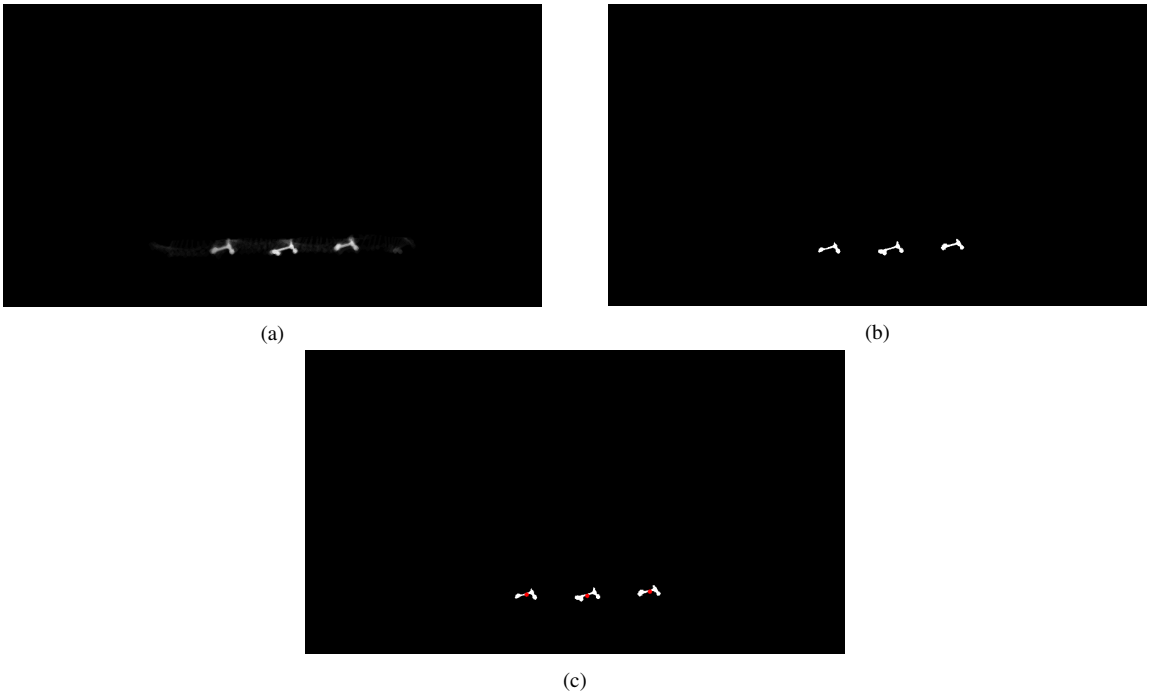

(a) (b)

(c)

Figure 4.12: Method to identify flat foot positions in a walking sequence: a) GTI representing feet evolution over time; b) All flat foot events after applying the Otsu's threshold; c) Flat Foot positions determined by the centroids.

Once flat foot centroids had been determined, spatial parameters were estimated. Starting with step length, which is basically the distance between two consecutive initial contacts, it was estimated as the distance covered between two consecutive flat foot events. Due to the lack of depth information from a 2D camera, there can be a difference between the scales of the two feet and so, to minimize errors, the developed algorithm computed the euclidean distance between flat foot centroids expressed in pixels. Since individuals have different heights, which can influence their step length, for comparison purposes, the step length was normalized with respect to their height — expressed in pixels —, as shown in equation 4.3. This normalization resulted in a dimensionless step length.

$$StepL = \frac{euclidean\_distance(FF\_centroids_i : FF\_centroids_{i+1})}{height} \tag{4.3}$$

where i and $i+1$ are consecutive indices of the $FF\_centroids$, with i between 1 and the total number of

flat foot centroids estimated in a video sequence.

Step length symmetry can then be estimated as the absolute difference between right and left step lengths, i.e., consecutive step lengths, according to equation 4.4.

$$StepL_{symmetry} = |StepL_{i+1} - StepL_i| \tag{4.4}$$

where *i* and *i+1* are consecutive indices of the *StepL*, with *i* between 1 and the total number of step lengths estimated in a video sequence.

Stride length can be defined as the distance travelled during a gait cycle. It was also estimated using the obtained step length, since two consecutive steps lengths are equivalent to a stride length, as demonstrated in equation 4.5. Since stride length is computed using step length, is, as well, dimensionless due to previous height normalization. This applies to any other feature that relies exclusively either on the step length or stride length for its computation, such as step and stride length symmetry.

$$StrideL = StepL_i + StepL_{i+1} \tag{4.5}$$

where *i* and *i+1* are consecutive indices of the *StepL*, with *i* between 1 and the total number of step lengths estimated in a video sequence.

To calculate stride length symmetry, a video sequence needs to contain more than one gait cycle, in order to be possible to obtain a stride length from both feet, unlike $StepL_{symmetry}$ for which one cycle is enough to have information from the two feet. Meeting this criteria, this measure was estimated following equation 4.4, by replacing *StepL* for *StrideL*.

Variability was determined by computing a commonly known coefficient of variation *(CV)*, defined as 4.6, using information from stride lengths during gait cycles. This coefficient is obtained by calculating the standard deviation (std) and dividing by the mean of the considered variable, *StrideL*. Then it is multiplied by 100% to obtain the result as a percentage, according to 4.6.

$$CV = \frac{std(variable)}{mean(variable)} \times 100\% \tag{4.6}$$

Subjects' velocity was estimated by dividing the distance travelled during the video sequence by the duration of the sequence, as in equation 4.7. The duration of the video sequence expressed in seconds, *period*, was defined as the time between the first and the last initial contacts that were registered, while the distance was calculated as the sum of step lengths of the considered sequence. Since the step length is dimensionless, speed is expressed in s^{-1}.

$$Speed = \frac{Distance}{Period} \tag{4.7}$$

For a certain gait cycle, two double support phases can be detected, starting at the moment of initial contact and ending at the moment of toe off (TO). In order to extract temporal parameters from the video sequences, besides determining initial contact frames, it is necessary to detect TO events during the gait cycle. The developed algorithm detected TO by selecting a set of candidate frames in which this event is more likely to occur. The toe off event happens after the initial contact during the double support phase, when both feet are in contact with the ground, so candidate frames were selected between a maximum feet width (= initial contact) and a mean feet width (= mean equals to 0, due to normalization of feet width), as represented in Figure 4.13. For each double support phase, a set of toe off candidate frames can be determined.

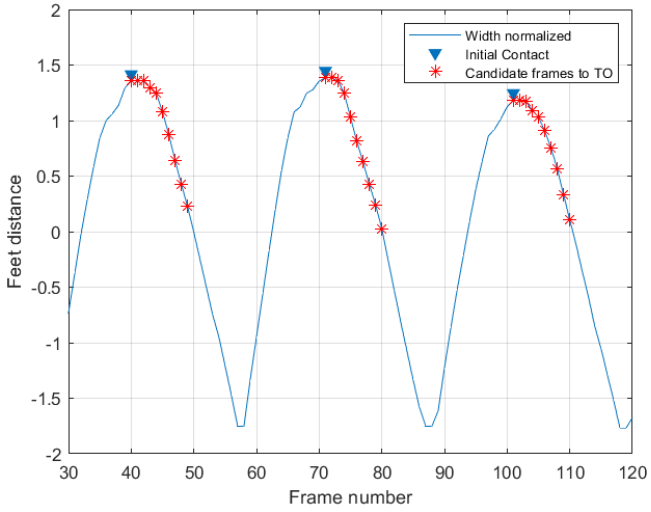

Figure 4.13: Candidate frames to TO detected between maximum feet width(=IC) and mean feet width.

The toe off occurs twice per gait cycle, to the foot that is not flatted during the double support phase, as represented in Figure 4.14c. The estimation of a TO event was performed by computing the overlap between consecutive flat and TO positions to the same foot. This reflected in overlapping each TO foot candidate with the flat foot that occurred immediately before, as exemplified in Figure 4.14.

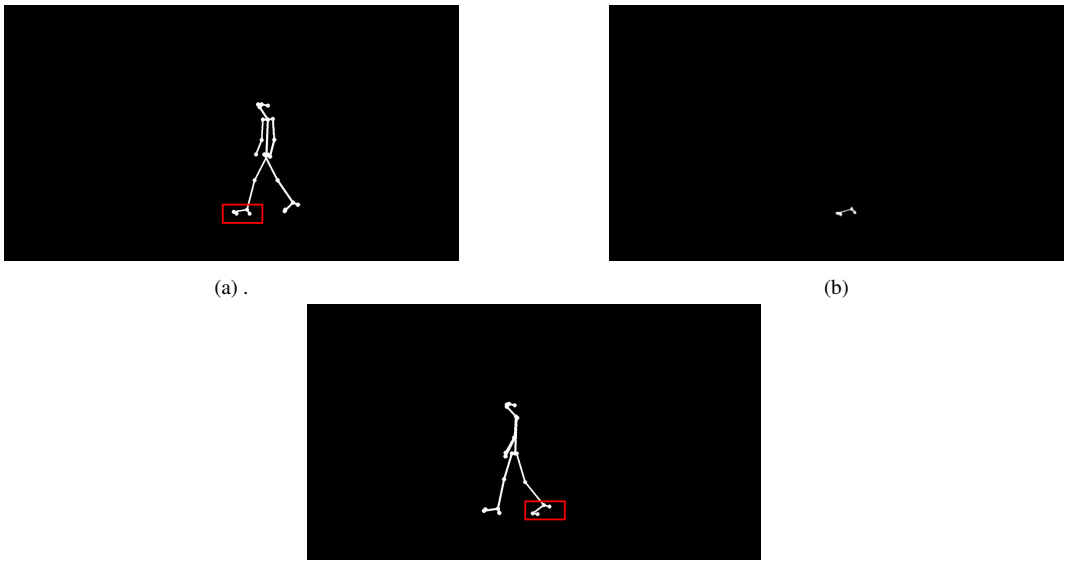

(a) .

(b)

(c)

Figure 4.14: Exemplifying frames to compute the overlap between consecutive flat and TO positions to the same foot. a) Represents the flat foot that occurred immediately before the considered TO; b) Respective flat foot image for the overlap computation; c) TO foot of one of the candidate frames of the correspondent set.

The overlap between TO and flat foot for the same foot was computed as the percentage of the TO foot covered by the flat foot. Determining the TO frame was completed by choosing the first frame where the overlap between consecutive flat foot and TO foot candidate was about 30%. Looking for the TO and FF positions to the same foot, implies selecting the FF position immediately before to the TO occurrence. So, considering the example in Figure 4.15, to detect the TO_2 frame right after IC_2, the flat $foot_1$ image that occurred after the IC_1 and during double support $phase_1$ was overlapped with every TO foot in each candidate frame of the set_2, in which the first that presented a overlap about 30% was selected as TO

frame, the frame when the toe is still in contact with the ground (toe off position) — the third represented in Figure 4.15c.

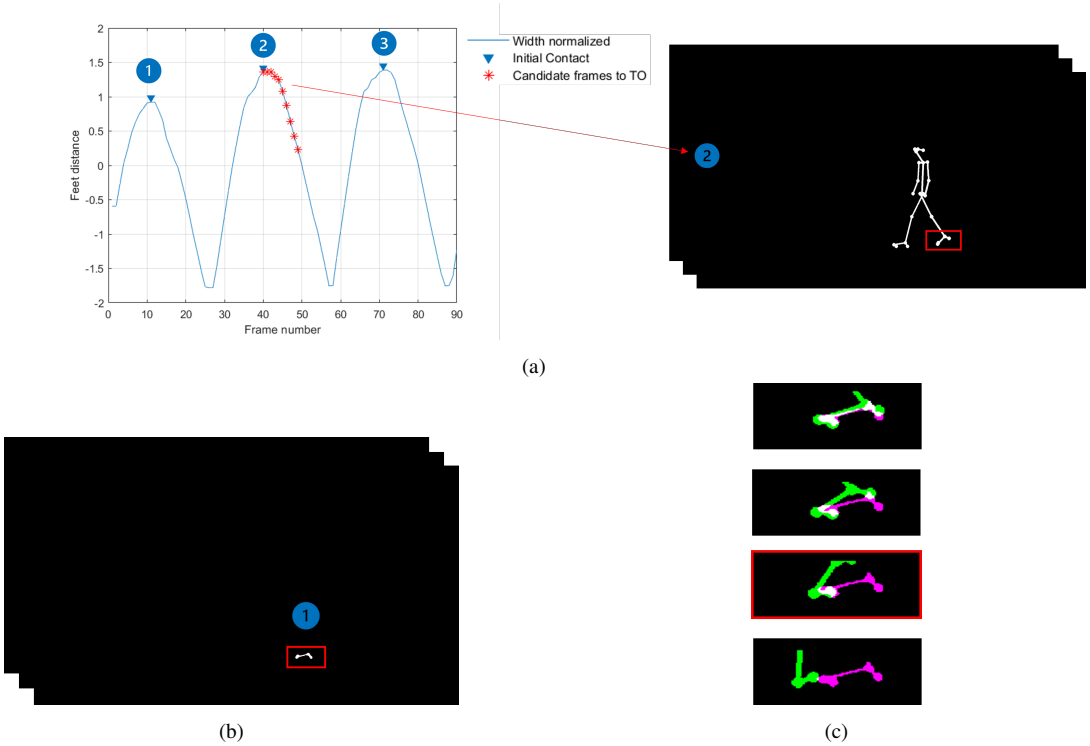

Figure 4.15: Steps to determine TO frame, giving as example the TO after IC_2. a) In the left side, plot representing initial contacts during a gait cycle and respective candidate frames to IC_2; in the right side, example of one of the candidates TO frame with TO foot being selected to overlap; b) Flat foot image to the same foot, FF_1, occurred immediately before and selected to overlap with each TO candidate of every frame of the correspondent set; c) Overlap with FF_1 and TO_2 foot candidates. White represents the overlap, rose represents the area occupied by flat foot and green represents the area occupied by the TO candidate. The red bounding box indicates when the overlap is about 30%.

Once TO frame was detected, temporal parameters such as double support time, pre-swing time, stance time and gait cycle time were estimated for each gait cycle of the video sequence. Since a video sequence contains multiple gait cycles, multiple feature values can be computed, which can then be used to compute an average value of the feature. All these parameters were expressed in seconds, hence each feature was divided by the frame rate (fps = 50) of the video sequence.

Double support time was defined as the time that both feet are in contact with the ground and can be measured as the duration of the two double support phases that occur during a gait cycle. Each phase starts at the IC and ends at the TO, so the time between these two occurrences is the duration of each double support phase. According to 4.8, double support time was computed as the sum of the differences between IC frame and TO frame for each phase.

$$Double\_support\_time = \frac{\sum_{i=1}^{N} TO_i - IC_i}{frame\_rate} \tag{4.8}$$

where N is the number of double support phases per a gait cycle (i.e N=2) and i is the index of the double support phase considered.

The second double support time, immediately before the swing phase, can also be denominated as pre-swing time. In this sense, pre-swing time was defined as the second double support period of a gait

cycle, according to the following equation 4.9:

$$Pre\_swing\_time = \frac{TO_2 - IC_2}{frame\_rate} \tag{4.9}$$

with *2* representing the TO and IC indices belonging to the second double support phase on the gait cycle.

It is during the stance phase that both double support phases take place. Stance phase is the period of the gait cycle when the observed foot is in contact with the ground, and it starts with a double support period, followed by a single support of the flat foot and a last double support period before starting the next gait phase. Knowing that a double support phase ends with a TO occurrence, stance time can be estimated as the time between the first IC and the second TO registered on a gait cycle, as represented in equation 4.10.

$$Stance\_time = \frac{TO_2 - IC_1}{frame\_rate} \tag{4.10}$$

where *2* and *1* correspond to the indices of the TO and IC considered in a gait cycle.

The last temporal parameter that was estimated was gait cycle time, which is defined as the duration of a gait cycle, and thus, computed as the difference between first and last initial contact frames, according to 4.11.

$$Gait\_cycle\_time = \frac{IC_3 - IC_1}{frame\_rate} \tag{4.11}$$

where *1* and *3* are the indices of the IC considered in a gait cycle.

Regarding body-related-features, they were estimated considering all body information and positioning during an entire gait cycle. This information was acquired by using the computed SGEIs for the estimation of body features. Using the SGEIs provides robustness to variations occurring at different instants of the gait cycle for both shift of CoG and Torso Orientation (TOR).

The shift of CoG was measured as the displacement between the center of gravity and the center of support, as illustrated in Figure 4.16. For this estimation, CoG was obtained as the weighted centroid of the SGEI, and CoS as the weighted centroid of the feet region by selecting the bottom 10% of the SGEI. The weighted centroids can be described as the center of a region based on pixels' location and intensity values of the SGEI.

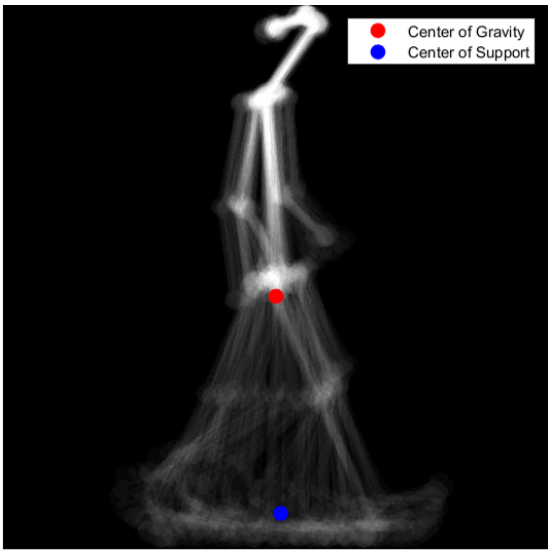

Figure 4.16: SGEI with center of gravity and center of support identified. At blue is represented the centroid of feet region and at red the center of gravity of the entire SGEI.

The proposed algorithm computed shift of CoG for every gait cycle as the absolute difference between the horizontal coordinates of the CoG and CoS, expressed in pixels, according to 4.12.

$$CoG_{shift} = |CoG_x - CoS_x| \tag{4.12}$$

The last body-related feature, denominated as torso orientation, was also computed using the SGEI for the entire gait cycle. The computation of TOR was done by using *regionprops* function of MATLAB, which receives as input the SGEI and calculates the TOR as the angle between the x-axis (blue dashed line) and the major axis of the ellipse that surrounds the upper body region. Both the ellipse and the x-xis are estimated within *regionprops* function, but were illustrated in figure 4.17 for a matter of exemplification.

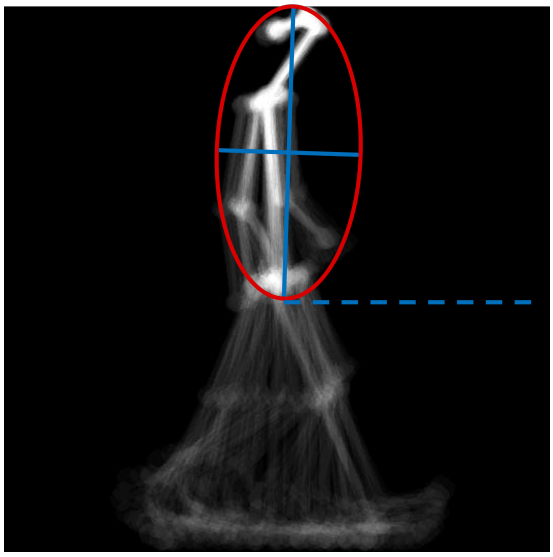

Figure 4.17: TOR computation example, with the blue dashed lines representing the x-axis and blue straight line representing red ellipse's axis.

4.4.2 TUG Features

Using the skeletons obtained from the TUG test sequences, other parameters to evaluate fall risk were estimated. Considering the main phases of the TUG test (getting up from the chair, walking, turning and sitting), the following time parameters were estimated by measuring the duration of execution of these phases. The definition of each phase of the TUG test was based on the kinematic description of each task available in [63]:

- **Sit-stand time (s):** It corresponds to the time to move from sitting to standing position. It starts with initiation of forward trunk lean and ends with end of vertical movement of the upper body.
- **Turn-around time (s):** It corresponds to the time needed to turn 180º degrees and to be in position to start walking back towards the chair. It starts with mid-stance of the final step of walking phase and ends with mid-stance of the first step after turning.
- **Turn-sit time (s):** It corresponds to the elapsed time between turning and sitting back on the chair.
- **Stand-sit time (s):** It corresponds to the time it takes the subject to sit back on the chair from the standing position. It starts with beginning of pelvis rotation before lowering to the chair and ends with end of vertical movement of the upper body.
- **Walk time (s):** It corresponds to the total time needed to walk the established 3 meters, back and forth. It can be divided into two periods: i) between end of sit-to-stand and start of turn-around and ii) between end of turn around and start of stand-to-sit.
- **TUG time (s):** It corresponds to the total time it takes to complete the entire TUG test. It starts and ends with the subject seated in the chair.

Following the previous definitions, the frames corresponding to the beginning and to the end of each phase were determined. Starting with **sit-stand time**, it was estimated as the difference between the first frame of the video sequence and the stand frame. The stand frame was defined as the frame corresponding to the standing position, when the subject reaches his/her first height local maximum before his/her first initial contact. To identify the stand frame, the height of the skeleton was computed over time and the first local maximum was determined, thus representing the ending of vertical movement of the upper body. It was ensured that this frame corresponded to a moment before the first initial contact.

Turn-around time was estimated as the time difference between the pre-turn frame and the post-turn frame. Both frames were detected by computing feet width over time, as done before when estimating feet related features. Pre-turn frame corresponds to the frame immediately before the subject starts the turning movement and it was defined as the frame representing the mid-stance phase of the gait cycle, which approximately happens when the distance between feet is minimum. This was done by computing the minimum distance between feet over the video sequence and choosing the last minimum distance occurrence immediately before turning. To determine post-turn frame, the approach was similar. Post-turn frame is the frame that ends the turn-around phase, and corresponds to the first mid-stance after turning. It was defined as the first minimum of the feet distance with the subject turned towards the chair.

Stand-sit time was estimated as the time difference between the pre-sit frame and the sit-frame, which is the last frame of the TUG sequence. Pre-sit frame was estimated also by looking for the mid-stance frame before turning, which will approximately correspond to the moment when pelvis starts the rotation. The frame with the last minimum distance between feet, immediately before starting to turn to sit back to the chair, was selected as the pre-sit frame.

Walk-time and turn-sit time were estimated using the previously detected frames. The first period of walk-time was defined as the time difference between the stand frame and the pre-turn frame, while the second period was defined as the time difference between the post-turn frame and the pre-sit frame. **Turn-sit time** was determined as the time difference between the pre-turn frame and the sit frame.

Finally, the **TUG time** was estimated as the time difference between the first and last frames of the video sequence.

The illustration of each of these frames is presented in Figure 4.18.

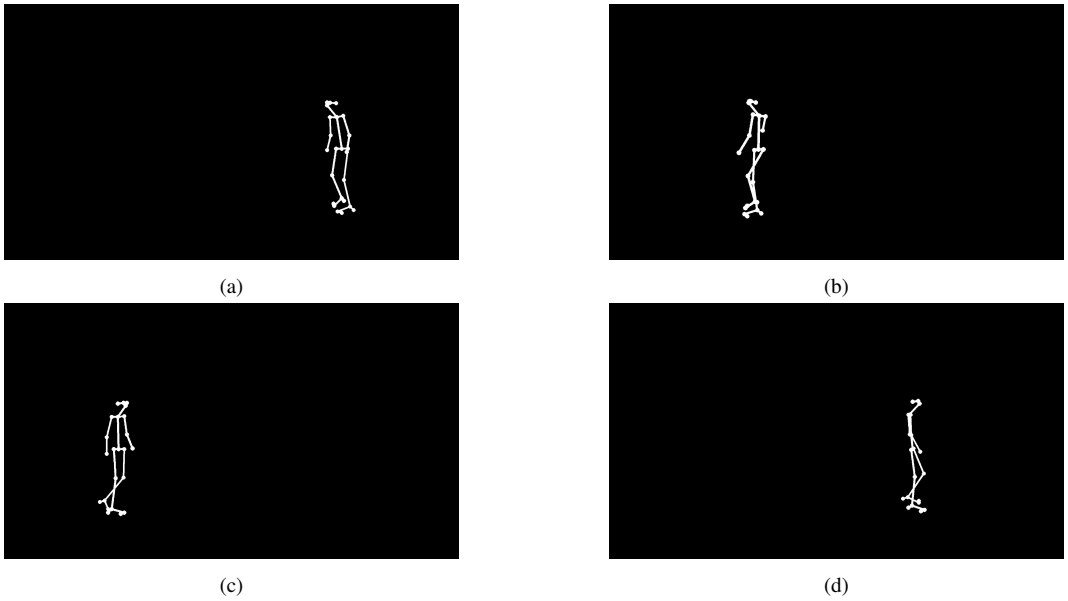

Figure 4.18: Frames representing main events during TUG test. a) Stand frame; b) Pre-turn frame; c) Post-turn frame; d) Pre-sit frame.

Apart from these temporal parameters, the following gait features were estimated during the walk-time:

- **Step length:** This feature is the mean of normalized step lengths registered during both walking directions, excluding the last step in both walk phases — dimensionless.
- **CV Step length (%):** This feature is the mean of the coefficient of variation for the step length during both walk directions — expressed in %.
- **Speed (s^{-1}):** This feature corresponds to the average speed registered during both walking directions — expressed in s^{-1}.
- **Number of steps:** This feature indicates the total number of steps registered during the entire test — dimensionless.

Except for the number of steps, the explanation of how the previous parameters are computed was provided earlier in this chapter. The number of steps was estimated as the number of initial contacts that occurred during the entire sequence, with each new initial contact corresponding to a new step.

4.5 Validation of Gait Time Parameters with Control Group

After concluding data collection with the control group at ESSCVP, the video sequences regarding the walking activity were submitted to a process of validation. This step consisted of extracting gait time

parameters from video sequences using *Contemplas* Video Analysis Software [3] with the objective of later comparing these parameters with those extracted using the developed algorithm for the same sequences. *Contemplas* was designed to perform motion analysis in different situations, whether walking or running, with focus on building applications for clinical use. During the analysis, it offers the possibility of using only static images or an entire video sequence. In this study, the module for 2D markerless gait analysis was applied.

Since this estimation of parameters using *Contemplas* happened right after data collection, it was before occurring Data Organization in Section 4.3.1 and dividing the videos between sides. So, for every subject, the two initial videos recorded were analyzed and from each video only two gait cycles were selected, one from each side, in order to have information from both left and right sides of the subject's gait. A video sequence normally contains several gait cycles, but on this case only one gait cycle from each side was evaluated. This resulted in extracting a total of 4 parameters per gait cycle and 16 per subject — two videos, four gait cycles, four parameters per gait cycle, 16 parameters for one subject. *Contemplas* was available at the facilities of ESSCVP and the physiotherapist was responsible for this task, which comprised uploading each video to the software, selecting the time instant when the gait cycle events the software requested occurred, namely heel strike (initial contact), toe off, mid-stance and maximum knee flexion, and then repeat it for the gait cycle from the opposite side. At the end, the software gives as output a report with time parameters estimated for both left and right sides of the uploaded video sequence, as reported in Figure 4.19. The time parameters measured by the *Contemplas* that were selected for validation were gait cycle time, stance phase time, double support phase time and second double support phase time, also named pre-swing time.

For this validation stage it was important to select the same gait cycles that the physiotherapist selected during gait analysis with the *Contemplas* software, so that comparison between parameters of both systems — developed algorithm and *Contemplas* — happened in the correct way. When validation was complete, there was no need to compute gait parameters only for the same gait cycles previously selected, but instead to consider the remaining gait cycles in the video, after discarding the first and last cycles as mentioned in Section 4.3.1.

[3] https://www.mar-systems.co.uk/contemplas-video-analysis-software/

Clinical gait analysis (1 camera)

Date: 12/07/2021

Sara Ponte

Born:

ESS LISBOA

Distance-time parameters

Gait parameters

Distance-time-parameters	Left side		Right side	
Gait cycle	1,060s		1,060s	
Stance phase	0,620s	58,5%	0,660s	62,3%
Swing phase	0,440s	41,5%	0,400s	37,7%
Single support phase left	0,440s	41,5%	0,400s	37,7%
Single support phase right	0,440s	41,5%	0,440s	41,5%
1st double support phase	0,100s	9,4%	0,120s	11,3%
2nd double support phase	0,080s	7,5%	0,100s	9,4%

Figure 4.19: *Contemplas* output after markerless video gait analysis, with representation of the gait time parameters estimated.

Chapter 5

Results and Discussion

In this chapter, the major results of analyzing 2D acquired video data to assess fall risk are discussed. Section 5.1 starts with the results concerning the first pre-processing step, which was the extraction of skeletons for every frame of the video sequences. Section 5.2 presents the outcome of the two stages of validation proceeded with the control group — *Contemplas* software, for walking sequences, and Manual, for TUG test sequences. Finally, Section 5.3 provides the results regarding the computation of fall risk indicators for the control and elderly group.

5.1 Skeleton Extraction

2D skeletons were obtained for every single frame of the considered video sequences using OpenPose library. Giving as input raw video sequences from both activities (i.e., walking activity and TUG test), OpenPose returned videos with tracked human skeletons for every time instant. Each skeleton frame contained in the video sequence was then converted into a binary image. Exemplifying results from this pre-processing stage are shown in Figure 5.1.

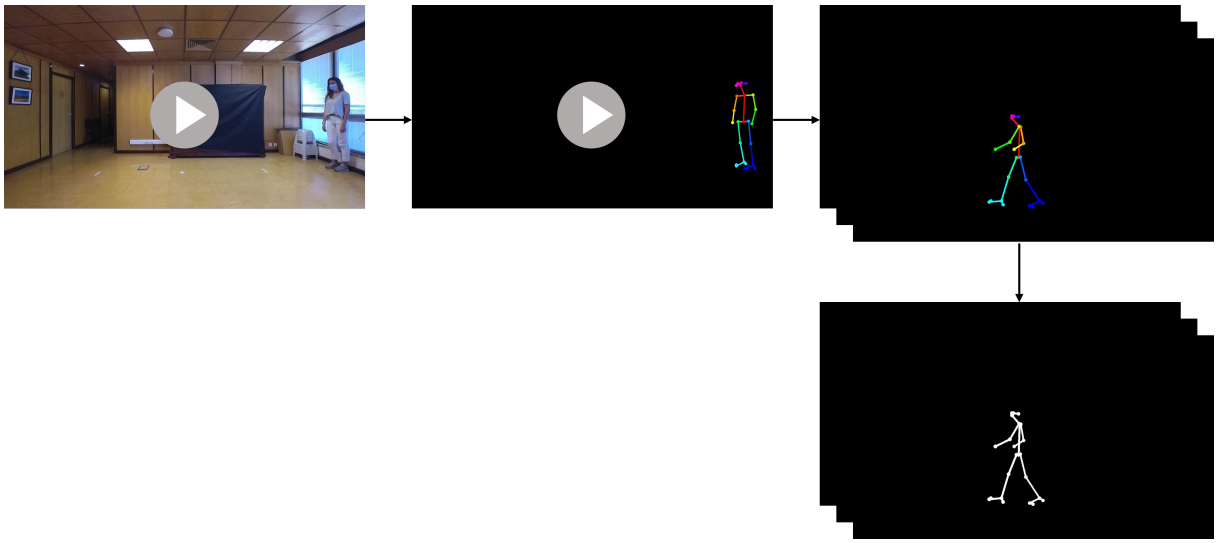

Figure 5.1: Results of skeleton extraction steps: 1st image represents one of the video inputs to OpenPose software, 2nd image represents the correspondent video output, 3rd image represents the containing frames of the video sequence, and 4th image represents the containing frames after converting into binary.

As mentioned earlier, the video-camera used for the acquisitions was previously defined with a resolution of 1080p, which allowed to obtain skeletons with a high accuracy. Evidence [64] shows that

cameras with poor resolution result in lower accuracy in tracking skeletons from human body, hence choosing this resolution resulted in fewer errors. However, the higher the resolution, the longer it takes for the OpenPose to give an output. Another factor that influences the time to obtain a output it is the number of frames per second, where the higher the number of frames of the video-camera, the longer the time to run OpenPose. As default, the video-camera used had 50 fps. So, depending on the required, the choice must be balanced between these three variables (resolution, fps, time). In this case, OpenPose was executed in a AMD Ryzen 7 4700U CPU (8-core), with 8GB of RAM.

Considering the data acquired from the 29 young subjects from the control group, only two, S11 and S19, were discarded and not used for analysis due to a higher incidence of skeleton extraction errors. Illustrations of the common errors that occurred in skeleton extraction from the video sequences of S19 and S11 can be found in Figure 5.2.

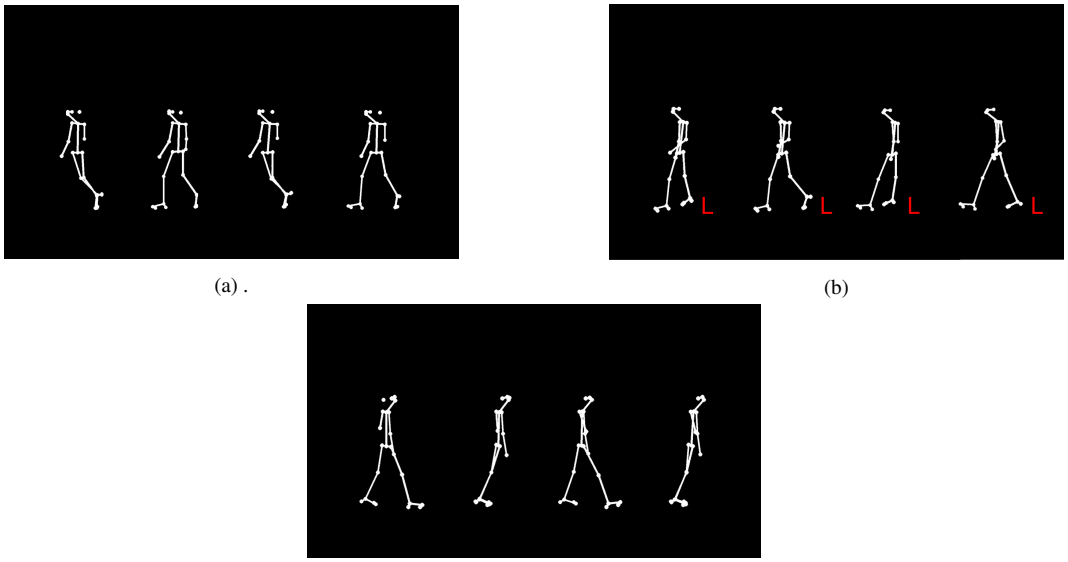

(a) . (b)

(c)

Figure 5.2: Examples of common skeleton extraction errors that occurred in consecutive frames of a certain sequence. a) Example of errors in the estimation of leg positioning on S19 sequences; b) Example of errors in the positioning of left (L) leg on S19 sequences, by not following the normal periodic movement; c) Example of errors in leg positioning on S11 sequences.

This type of errors did not occur exclusively in these discarded subjects. The remaining subjects also presented, occasionally, some parts of the skeleton that were missing, but the algorithm was robust enough to handle some isolated errors, while on the videos that were discarded those errors happened more often, making it impossible to choose one entire gait cycle without estimation errors.

The reason why this happened was easier to explain for S19 than for S11. During the acquisition, S19 was wearing a long skirt, which occluded both inferior members, as shown in Figure 5.3. By occluding both legs, the skirt made it difficult for the OpenPose to identify accurately their current positioning on every single frame over time, resulting in some of the errors demonstrated in Figure 5.2a and 5.2b.

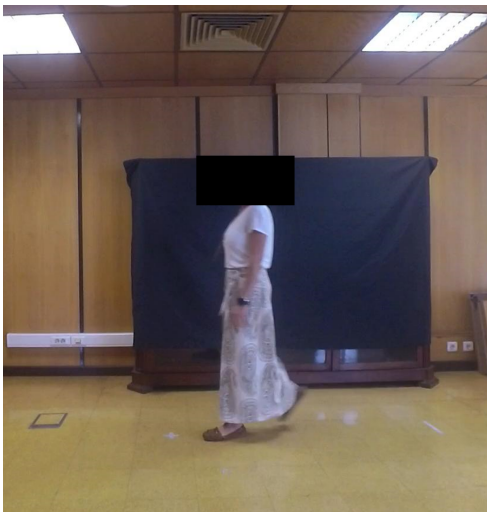

Figure 5.3: Subject #19

As for S11, what made it inappropriate for analysis when comparing it to other subjects, was the fact that it was not possible to select a single gait cycle without any consecutive errors, like the ones exemplified at Figure 5.2c.

On the second phase of acquisitions, with the elderly, there was a higher number of discarded subjects. Data was initially collected with fourteen elderly, but only 6 subjects were suitable for analysis. The fourteen subjects were all female, and most of them participated using medium-long skirts. During the first phase of acquisitions, with the control group, it became clear that subjects who wear long skirts would be a source of errors in the estimation of the skeletons. However, at the same time, it was something that was not possible to avoid since the elderly came to the acquisition session wearing the clothes they chose. In this way, wearing medium-long skirts or dresses worked as subjects' exclusion criterion. Figure 5.4 is an example of one of the elderly excluded from the analysis. The skeletons of the discarded subjects presented the same type of errors as the ones previously presented in Figure 5.2.

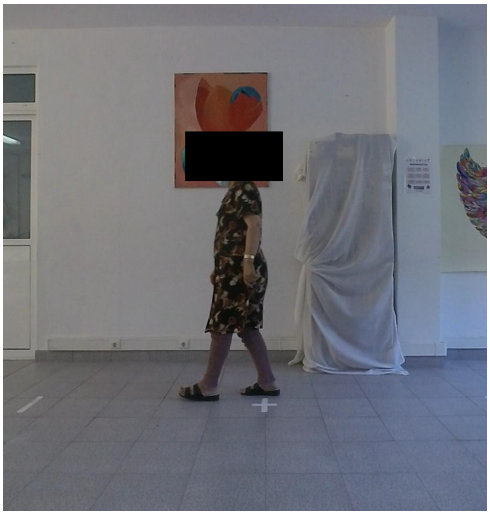

Figure 5.4: Example of one of the elderly excluded from the analysis.

5.2 Validation of Control Group

5.2.1 Validation of Gait Time Parameters with *Contemplas* Software

The developed algorithm detects TO and IC events to estimate temporal gait features. So, after estimating these parameters for the gait cycles previously analyzed with the *Contemplas*, a comparison between parameters obtained from the two systems — Developed algorithm and *Contemplas* software — was performed. Since TO and IC events were manually identified on each gait cycle by the physiotherapist during the *Contemplas* analysis, an error margin of ± 1 frame with respect to the *Contemplas* was allowed. With a frame rate of 50 fps (i.e., 0.02 s per frame), this reflected as having an uncertainty associated to the estimation of every time parameter, as shown in Table 5.1.

	Formula*	**Uncertainty**
Gait cycle time (s)	IC_3 - IC_1	± 0.04
Stance time (s)	TO_2 - IC_1	± 0.04
Double support time (s)	(TO_1 - IC_1) + (TO_2 - IC_2)	± 0.08
Pre-swing time (s)	TO_2 - IC_2	± 0.04

Table 5.1: Uncertainty associated to the estimation of temporal features.

*divided per frame rate

This validation stage consisted in verifying if the parameters estimated by the algorithm were close to the ones obtained by the *Contemplas*, and when this happened it was counted as a correct case. A correct case means that the parameters estimated by the algorithm were within their uncertainty range. As an example, considering the case that $\text{StanceTime}_{contemplas} = 0.68$ s, this means that for $\text{StanceTime}_{algorithm}$ to be counted as a correct case it needs to be within the range of 0.68 s $\pm$ 0.04.

For validation purposes, accuracy score was calculated for every parameter along all subjects, following equation 5.1.

$$Accuracy = \frac{\#Correct\_Cases}{\#Total\_Cases} \tag{5.1}$$

Apart from that, the mean difference was estimated between the parameters obtained from both systems, as shown in table 5.2.

	Accuracy (%)	**Mean$_{Algorithm}$ (s)**	**Mean$_{Contemplas}$ (s)**	**Mean Diff (s)**
Gait cycle time	94.4%	1.08	1.10	0.2
Stance time	91.7%	0.69	0.67	0.02
Double support time	93.5%	0.23	0.23	0.00
Pre-swing time	87.0%	0.13	0.12	0.01

Table 5.2: Comparison between temporal gait features estimated by the developed algorithm and the ones obtained with the *Contemplas* software to all subjects of control group.

Table 5.2 shows an accuracy ranging from 87% to 94% when using an algorithm developed in MATLAB for the detection of IC and TO events and consecutive estimation of time parameters. The higher accuracy for gait cycle time could be related to the fact that this parameter only depends on the estimation

of IC, while the other parameters depend on both IC and TO, which doubles the chances of estimation errors occurring and consequently having lower accuracy. Regarding mean difference results, they support the idea that the developed algorithm can estimate, for a determined group of subjects, temporal gait features that are on average very close to those estimated by the gait analysis *Contemplas* software.

When comparing the estimated time parameters with those measured by a pre-validated software designed for gait analysis, the results look very promising. One of the principal advantages of developing a algorithm which estimates TO and IC events and then computes temporal features, homologous to *Contemplas*, is that a computer vision method can do it automatically, while *Contemplas* includes a manual component in their analysis (identification of gait cycle events such as TO and IC).

With the accomplishment of this validation stage, ensuring that the two systems share similar measurements, the second phase of acquisitions, with the elderly, was completed only using the developed algorithm for the estimation of gait parameters.

5.2.2 Validation of TUG Test Features

Similar to what was done with gait time parameters, TUG features were also validated. Since the *Contemplas* software was not a option because it does not provide this type of evaluation, TUG parameters obtained by the algorithm were validated using two approaches: first, validation with manual estimation, to check if there was a huge discrepancy between parameters obtained manually and automatically; if not, it meant that the algorithm was computing them correctly. The second approach was to verify if the TUG parameters estimated were within the expected range for a group of young adults. This was achieved by comparing the average group parameters obtained with those available at literature.

The first stage consisted in looking at every TUG test video and defining manually where each phase of the TUG test started and ended, based on the definition previously given in Chapter 4.4.2. Video labeling was a time-consuming task, but once accomplished, the estimation of TUG parameters was pursued by subtracting the time instants that delimit each interval, except for the TUG test time, since it was the complete time duration of the video. After manual estimation, for every subject, each parameter was compared with the ones measured by the algorithm. This comparison was assessed by computing a correlation coefficient between values obtained with each method and a mean difference for each method, as represented at Table 5.3.

	Correlation Coefficient	**Mean$_{Algorithm}$ (s)**	**Mean$_{Manual}$ (s)**	**Mean diff (s)**
Sit-stand time	0.99	1.21	1.22	0.01
Turn-around time	0.86	1.39	1.37	0.02
Turn-sit time	0.98	6.39	6.38	0.01
Stand-sit time	0.91	2.41	2.40	0.01
Walk time	0.95	5.50	5.51	0.01

Table 5.3: Comparison between TUG time parameters manually estimated and those automatically computed for control group subjects.

Correlation coefficients whose magnitudes are above 0.8 normally indicate a strong correlation between the two variables being compared. Results in Table 5.3 show that the computed coefficients are all above 0.8, meaning that it is possible to estimate TUG time parameters automatically from video sequences with these same parameters being very close to the ones measured manually. Mean difference

results between the two strategies also sustains the possibility of extracting TUG time features with a computer vision algorithm.

After studying the hypothesis of estimating TUG parameters automatically, the measured features were compared with a study from the literature, as shown in Table 5.4. Comparison with other published studies sometimes can be difficult either due to sharing different TUG conditions or due to interval definitions not corresponding to the ones considered. In this case, the study developed by Beyea et. al [65] also recruited young adult subjects (aged between 21-64), and defined the same TUG phases. The only clear difference was that Beyea et al. subdivided into two phases the i) walk time: walk#1 and walk#2 and ii) stand-sit time: Turn#2 and stand-to-sit, while on this current thesis these two phases were estimated and considered as a whole. For a matter of comparison, each sub-phase of the study was summed, to be equivalent to the walk time and stand-sit-time considered in this thesis, as demonstrated in Table 5.4.

	This study	**Beyea et al. [65]**
	Control Group ($mean \pm std$)	Healthy Subjects ($mean \pm std$)
Sit-stand time (s)	1.21 ± 0.18	1.25 ± 0.30
Turn-around time (s)	1.39 ± 0.29	1.31 ± 0.24
Stand-sit time (s)	2.41 ± 0.40	$2.68 \pm 0.53^{*}$
Walk time (s)	5.50 ± 0.77	$5.68 \pm 1.10^{*}$
TUG time (s)	10.51 ± 0.98	10.82 ± 2.33

Table 5.4: Comparison of TUG time parameters with a similar study from the literature.

*divided into two sub-phases each, so standard deviation was estimated following rules of propagation of errors.

Table 5.4 demonstrates that the parameters extracted using the developed algorithm are in agreement with the parameters obtained for a group which shares the same characteristics as the control group. This evidence can provide insight that the parameters estimated are within the expected range for young adult subjects, and therefore their estimation is being done correctly and according to what is expected.

This process of validation shows that a system that estimates correctly and automatically TUG test features can also provide additional information compared to what it is acquired during a traditional observational assessment by physioterapists. Besides measuring the total time to execute the TUG test, as physiotherapists usually do, this developed algorithm also measures other parameters like sit-stand time, turn around time, etc, which in a certain way quantifies what is only visually observed.

5.3 Comparison between Control Group and Elderly Group

Twenty-two parameters were computed for all subjects, twelve obtained from the walking sequences and ten from the TUG test sequences, as demonstrated in Table 5.5. Data analysis was focused on evaluating if there was statistical differences between young adult subjects with no risk of falling and elderly subjects who had risk of falling. To do that, usually one of the first steps is to test the normality of the data, but since one of the populations is limited in size [66], being composed of only a total of 6 subjects, a non-parametric test for two independent samples was directly applied instead.

Hence, for every parameter, a Wilcoxon Rank Sum test [67] was used to determine how well a given parameter can distinguish between control and elderly groups. The difference was considered significant when the parameter had a ρ-value below 0.05. Table 5.5 provides the results regarding the statistical test used for all parameters with their respective ρ-value, as well as means and standard deviations of each group.

Walking Sequences Parameters	**Control Group (n=27)** $mean \pm std$	**Elderly Group (n=6)** $mean \pm std$	**ρ-Value**
Step length	0.44 ± 0.03	0.32 ± 0.06	$<0.001^*$
Stride length	0.87 ± 0.06	0.64 ± 0.13	$<0.001^*$
Step length symmetry	0.03 ± 0.02	0.05 ± 0.03	0.034^*
Stride length symmetry	0.03 ± 0.02	0.04 ± 0.03	0.469
CV stride length (%)	2.77 ± 1.57	6.36 ± 4.39	$<0.001^*$
Speed (s^{-1})	1.16 ± 0.18	0.68 ± 0.22	$<0.001^*$
Stance time (s)	0.67 ± 0.05	0.71 ± 0.12	0.834
Gait cycle time (s)	1.09 ± 0.07	1.13 ± 0.13	0.834
Double support time (s)	0.24 ± 0.04	0.29 ± 0.09	0.129
Pre-swing time (s)	0.12 ± 0.03	0.15 ± 0.06	0.314
Shift on center of gravity (px)	3.62 ± 2.30	4.78 ± 1.70	0.118
Torso orientation (º)	86.68 ± 2.44	82.99 ± 4.11	0.003^*
TUG Parameters			
Sit-stand time (s)	1.21 ± 0.18	1.77 ± 0.67	$<0.001^*$
Turn-around time (s)	1.39 ± 0.29	1.53 ± 0.46	0.225
Stand-sit time (s)	2.41 ± 0.39	3.42 ± 1.17	0.009^*
Walk time (s)	5.50 ± 0.77	9.95 ± 3.44	$<0.001^*$
Turn-sit time (s)	6.39 ± 0.65	9.60 ± 2.89	0.002^*
TUG time (s)	10.50 ± 0.98	16.68 ± 5.22	$<0.001^*$
Number of steps	13.00 ± 1.51	21.67 ± 5.49	$<0.001^*$
Step length	0.43 ± 0.04	0.31 ± 0.05	$<0.001^*$
CV step length (%)	6.58 ± 4.61	12.60 ± 4.94	$<0.001^*$
Speed (s^{-1})	0.71 ± 0.09	0.45 ± 0.10	$<0.001^*$

Table 5.5: Means and standard deviations for the extracted parameters. * Statistically significant differences (ρ-Value < 0.05) between Control Group and Elderly Group.

According to Table 5.5, conducting a Wilcoxon Rank Sum test resulted in obtaining a total of 15 parameters with a ρ-Value below 0.05, which means that the values of the features estimated for the group of young adults with no risk of falling were significantly different from those estimated for the group previously evaluated with risk of falling. Also, all gait parameters that were significant for a ρ-Value = 0.05 were, as well, significant for a ρ-Value = 0.01, with step length symmetry being the only exception. In first hand, these results suggest that the developed algorithm is able to detect differences between the two groups under analysis.

Table 5.5 also reveals a greater incidence of discriminant parameters in the execution of the TUG test than in the performance of the walking activity (9 vs 6), which might indicate that the TUG test, in this context, can be more sensitive at detecting differences in gait. The fact that the TUG test requires

the subject to perform other types of tasks than just walking, like turning around and standing up from a chair, can help to better detect fall risk indicators that could not be as evident when asking the subjects to simply walk forward. Therefore, this suggests that the TUG test could work as a best fall risk evaluation method, at least between a group without risk and a group with increased risk. As an example, looking at the TUG test time, it is possible to see the difference in duration between executing the test as a control group subject and as an elderly with fall risk (10.50 vs 16.68, respectively), which is in agreement with a study published in BMC Geriatrics [41] that states that a TUG test duration of 13.5 seconds or longer can be a predictive of fall risk, and by contrast, a TUG score of under 13.5 seconds suggests a better functional performance.

When looking at mean and standard deviations values of significant features, the temporal parameters and number of steps of the elderly group increased significantly compared with those of the control group. This increase is followed by a decrease in their speed and in their step and stride length, meaning that the elderly with risk of falling take more time to execute a determined task or movement, which could be influenced by their fear of falling that normally leads the elderly to adopt a slower pace and smaller steps. Parameters regarding variability and symmetry, such as CV stride length, CV step length and step length symmetry also increased ($p<0.001$, $p<0.001$ and $p=0.03$, respectively) for the elderly group, revealing that these subjects when compared to the young adult subjects may exhibit more fluctuations during walking, thus having an impact in their step symmetry and variability.

Since only a small sample of elderly was enrolled in this study, there was a chance that the differences in the parameters between both groups would not be so clear. In order to be prepared for this eventual occurrence, during the fall risk evaluation, the physiotherapists noted aside the elderly subjects who presented major alterations in their gait at the motor level. This was done with the intention of later verifying if the developed algorithm could be sensitive to these gait changes when comparing with the control group. Table 5.6 reports this comparison between the young adult subjects group (n=27) and elderly with major gait alterations (n=2), using a Wilcoxon Rank Sum test, as previously.

Walking Sequences Parameters	Control Group (n=27) $mean \pm std$	Elderly w/ major gait alterations (n=2) $mean \pm std$	ρ-Value
Step length	0.44 ± 0.03	0.25 ± 0.05	0.023*
Stride length	0.87 ± 0.06	0.49 ± 0.09	0.023*
Step length symmetry	0.03 ± 0.02	0.05 ± 0.02	0.035*
Stride length symmetry	0.03 ± 0.02	0.03 ± 0.02	0.699
CV stride length (%)	2.77 ± 1.57	6.75 ± 3.57	0.043*
Speed (s^{-1})	1.16 ± 0.17	0.42 ± 0.11	0.023*
Stance time (s)	0.67 ± 0.06	0.86 ± 0.10	0.023*
Gait cycle time (s)	1.09 ± 0.07	1.29 ± 0.09	0.022*
Double support time (s)	0.24 ± 0.04	0.39 ± 0.09	0.022*
Pre-swing time (s)	0.12 ± 0.03	0.20 ± 0.06	0.022*
Shift on center of gravity (px)	3.62 ± 2.30	6.02 ± 1.69	0.053
Torso orientation (º)	86.68 ± 2.44	78.84 ± 5.52	0.028*
TUG Parameters			
Sit-stand time (s)	1.21 ± 0.18	2.47 ± 0.79	0.022*
Turn-around time (s)	1.39 ± 0.29	1.76 ± 0.65	0.043*
Stand-sit time (s)	2.41 ± 0.39	4.49 ± 1.62	0.023*
Walk time (s)	5.50 ± 0.77	14.07 ± 5.32	0.023*
Turn-sit time (s)	6.39 ± 0.65	12.53 ± 4.92	0.023*
TUG time (s)	10.50 ± 0.98	22.79 ± 8.65	0.023*
Number of steps	13.00 ± 1.51	27.67 ± 10.58	0.022*
Step length	0.43 ± 0.04	0.25 ± 0.15	0.023*
CV step length (%)	6.58 ± 4.61	16.26 ± 5.07	0.023*
Speed (s^{-1})	0.71 ± 0.09	0.33 ± 0.21	0.023*

Table 5.6: Means and standard deviations for the extracted parameters. * Statistically significant differences (ρ-Value < 0.05) between Control Group (n=27) and Elderly with major gait alterations (n=2).

This comparison resulted in a total of 20 parameters statistically significant for a ρ-Value < 0.05, with only shift of center of gravity and stride length symmetry not being significantly different. Comparing this analysis with the previous one that included all elderly subjects (see Table 5.5), five more discriminative parameters were obtained, adding to the previous 15. In fact, for the TUG test time, the mean difference between the control group and the elderly group doubled, pointing out that this subgroup of participants manifests more difficulties to complete the test.

These results could mean that, indeed, the developed algorithm was able to discriminate these alterations, and perhaps if the elderly population was larger, maybe the other subjects that did not present clear motor alterations — Elderly with minor gait alterations (n=4) — would not have so much weight on the average elderly group (n=6) and the differences would be more obvious, leading to more discriminant parameters, as this comparison showed. In addition, the number of significant parameters from the walking sequences shows that the walking activity is a better evaluation option when assessing risk of falling with individuals that present greater alterations in gait.

Nevertheless, the elderly with minor gait alterations were still evaluated as having risk of falling,

despite not showing these additional alterations during acquisitions. To check if the algorithm could still identify differences between this sub-group and the control group, a third Wilcoxon Rank Sum test was performed. Table 5.7 displays the results of statistical differences in the parameters between the two groups under analysis.

Walking Sequences Parameters	**Control Group (n=27)** $mean \pm std$	**Elderly w/ minor gait alterations (n=4)** $mean \pm std$	**ρ-Value**
Step length	0.44 ± 0.03	0.35 ± 0.03	0.003*
Stride length	0.87 ± 0.06	0.71 ± 0.07	0.004*
Step length symmetry	0.03 ± 0.02	0.05 ± 0.04	0.227
Stride length symmetry	0.03 ± 0.02	0.04 ± 0.03	0.536
CV stride length (%)	2.77 ± 1.57	5.98 ± 4.65	0.004*
Speed (s^{-1})	1.16 ± 0.18	0.79 ± 0.14	0.007*
Stance time (s)	0.67 ± 0.05	0.64 ± 0.04	0.205
Gait cycle time (s)	1.09 ± 0.07	1.05 ± 0.05	0.205
Double support time (s)	0.24 ± 0.04	0.24 ± 0.04	0.745
Pre-swing time (s)	0.12 ± 0.03	0.12 ± 0.03	0.789
Shift on center of gravity (px)	3.62 ± 2.30	4.27 ± 1.43	0.536
Torso orientation (º)	86.68 ± 2.44	84.46 ± 19.96	0.023*
TUG Parameters			
Sit-stand time (s)	1.21 ± 0.18	1.42 ± 0.27	0.009*
Turn-around time (s)	1.39 ± 0.29	1.41 ± 0.47	0.906
Stand-sit time (s)	2.41 ± 0.39	2.89 ± 0.76	0.093
Walk time (s)	5.50 ± 0.77	7.89 ± 1.48	0.005*
Turn-sit time (s)	6.39 ± 0.65	8.14 ± 1.50	0.023
TUG time (s)	10.50 ± 0.98	13.61 ± 2.16	0.006*
Number of steps	13.00 ± 1.51	18.67 ± 2.81	0.002*
Step length	0.43 ± 0.04	0.34 ± 0.03	0.003*
CV step length (%)	6.58 ± 4.61	10.78 ± 3.24	0.010*
Speed (s^{-1})	0.71 ± 0.09	0.51 ± 0.06	0.002*

Table 5.7: Means and standard deviations for the extracted parameters. * Statistically significant differences (ρ-Value < 0.05) between Control Group (n=27) and Elderly with minor gait alterations (n=4).

As expected, when comparing the elderly with minor gait alterations with the control group, it resulted in obtaining less significant parameters than the first and second comparisons, since this sub-group of elderly, among the others — Elderly group (n=6) and Elderly with major gait alterations (n=2) —, is the closest to the control group, even though sharing different risk evaluations. According to Table 5.7, a total of 13 parameters were significantly different between the four elderly and the twenty-seven young adult subjects. Parameters such as step length symmetry, turn-sit time and stand-sit time lost significance, meaning that these parameters could not be good indicators when the subjects under analysis have lower or no risk of falling.

A Pearson correlation coefficient was computed with the supplementary data acquired with questionnaires to understand if there was any linear relationship between age, sex, weight, height, Body Mass

Index (BMI), history of falls, use of walking aids, motor diseases and fall risk evaluation performed for both groups. Table 5.8 presents the obtained Pearson's coefficient for each variable.

	Pearson Correlation (rho)							
	Age	Sex	Weight	Height	BMI	History of falls	Walking Aid	Motor Diseases
Fall Risk	0.98	-0.27	0.20	-0.30	0.46	0.67	0.54	0.38

Table 5.8: Pearson's correlation coefficient between risk of falling and data from the questionnaire of both groups - age, sex, weight, height, BMI, history of falls, presence of walking aid and motor diseases.

The results regarding Pearson correlation show that age and history of falls are the only two variables with a coefficient above 0.6. As expected, age is the most strongly correlated with risk of falling (r = 0.98), since all subjects who were evaluated as having fall risk were older, thus resulting in a coefficient very close to 1. Among the elderly group evaluated with fall risk, the presence of registered falls in the past was also common, therefore being correlated with risk (r=0.67). The use of walking aid also reveals a correlation with fall risk, although weaker (r=0.57), and not necessarily a causal relationship. In other words, elderly can use walking aids as a support to walk and not being identified with risk of falling, and the opposite is also possible. The equivalent can be said about age, where increasing age increases the chances of developing fall risk, but, at the same time, a perfectly healthy elderly may not present any signs or indicators of fall risk.

To exemplify the appearance of a skeleton obtained for a young adult subject and for an elderly subject, Figure 5.5 illustrates consecutive skeletons extracted from a certain walking sequence for both groups under analysis.

(a) (b)

Figure 5.5: Visible differences between the skeletons of each group under analysis, control and elderly, respectively. a) Example of consecutive frames from a subject of control group; b) Example of consecutive frames from a subject of elderly group.

The principal visible differences between the skeletons from the two groups are step length and walking position. Figure 5.5b shows that the elderly takes smaller steps than a subject with no risk of fall and walks with a more curved and leaned posture. These two characteristics were assessed through a quantitative video analysis by computing parameters as step length and torso orientation, with both of these parameters being significantly different between the three comparisons performed (control (n=27) vs elderly (n=6), control (n=27) vs elderly with major gait alterations (n=2), control (n=27) vs elderly with minor gait alterations (n=4)). Apart from that, there are other changes that might not be so clear at naked eye observation or not be measured at all during an evaluation performed by a physiotherapist. Therefore, when using a computer vision algorithm, it can work as a complementary tool to the traditional method and help the physiotherapists to identify certain particularities that would not be acquired during a regular procedure.

Chapter 6

Conclusion

In this chapter, the major conclusions of developing a 2D vision-based method to assess fall risk is provided. Section 6.1 summarizes the general conclusions of this thesis and Section 6.2 introduces the main propositions for future work.

6.1 General Conclusions

With the increase in average life expectancy, the elderly population is increasing from year to year, and one of the most urgent problems to solve continues to be the occurrence of falls and their consequences. One way to act in the prevention of these episodes is to assess fall risk. However, clinical assessments have their own limitations such as the lack of quantitative information acquired during an evaluation predominantly based on the observational analysis of the healthcare professional, which may be subjective. In order to improve the current methodology, the present work proposed a quantitative system to assess risk of falling through gait analysis using 2D video data.

In this thesis, two phases of acquisitions were completed — one with a control group composed of young subjects and a second one with an elderly group composed of senior subjects who presented fall risk. Generally, data collection was successful, resulting in few errors when pre-processing video sequences to extract human skeletons. The only noticed concern was when subjects wore long skirts or dresses during video acquisition, which negatively influenced the accurate identification of inferior limbs position in each frame of the video, thus leading to skeletons with missing body segments. This method, compared to background extraction, simplified the acquisitions, with no need to worry about background heterogeneity, variance in luminosity and presence of shadows. In addition, having an easy installation process makes it suitable to replicate this data acquisition setup to other environments such as day-care centers and other elderly institutions.

The first objective of this work comprised verifying whether there was an agreement between the temporal gait parameters of the walking sequences measured by an algorithm developed in MATLAB and those measured by *Contemplas* software designed to perform gait analysis in a clinical context. With accuracy scores for every parameter ranging from 87% to 94% and with mean differences between both systems being approximately one-hundredth of a second, this confirms that the proposed algorithm can estimate, on average, and for a determined group of subjects, parameters very close to the ones estimated with *Contemplas* software. Hence, the development of an automatic and operational algorithm could be an equivalent to an expensive system that requires manual intervention for this type of analysis.

The second objective of this study was validating the time parameters estimated for the TUG test sequences, and this was achieved in two separate approaches — manual and literature validation. The

manually measured TUG parameters have proven to be strongly correlated with those measured automatically, obtaining a correlation coefficient value above 0.8. This correlation was aligned with mean differences results, since the maximum reached difference was only 0.02s and the minimum 0.01s. The estimated TUG phases duration was also compared with a study from the literature with similar characteristics and this comparison revealed that the obtained parameters were within the same range of the study. Both stages of validation suggest that the proposed algorithm provides reliable measurements of the TUG test parameters and that is possible to automatically measure the test duration, as well as other TUG test parameters that are not measured by physiotherapists during a regular TUG test.

The third objective of this thesis consisted of identifying parameters that could work as fall risk indicators for the elderly population. From the first global comparison between control and elderly groups, conducting a Wilcoxon Rank Sum test resulted in a total of 15 (out of 22) parameters with discriminative capability ($p<0.05$). Based on the large number of discriminant parameters associated to the TUG test, it can be inferred that it is a better tool to assess fall risk, when compared to the walking activity that only revealed to be sensitive in a group that presented greater alterations in gait. Additionally, the TUG test time estimated for the elderly group (= 16.67s) was in agreement with a study published in BMC Geriatrics which states that a duration of 13.5s or longer can be a indicative of fall risk. The second comparison between control group (n=27) and elderly with major gait alterations (n=2) allowed to perceive that the algorithm was capable of detecting the differences visually registered by the physiotherapists during the acquisitions. This was proven with an increase in the number of parameters that were statistically significant (20 vs. 15 out of the total 22 parameters) and with a greater mean difference in some of the computed parameters, such as TUG test time which doubled its mean difference. The third and last comparison demonstrated that statistical differences were detected between a sub-group evaluated with risk of falling but with less gait changes and a group with young adult subjects — Elderly with minor gait alterations vs Control Group. Although, as expected, it resulted in obtaining less significant parameters since that sub-group was the closest to the control group. These three analysis were always conducted comparing a control population with a small sample of elderly and so it is difficult to predict whether a greater sample would produce the same number of discriminant parameters. Or, otherwise, would lead to a higher number of individuals with similar characteristics to the elderly with major gait alterations, and this would translate into statistical differences in almost all parameters. Even working with only 6 elderly subjects, the results of comparing the two risk groups are promising and express the capability of the algorithm to identify fall risk indicators that reveal changes in gait, posture and in the performance of executing determined tasks as well. Lastly, the Pearson correlation between questionnaire data and fall risk classification, unsurprisingly, presented a strong correlation between age and risk of falling, but not necessarily implying a causal relationship. It is known that fall risk can be inevitably caused by age since increasing ages increase the chances of falling, but, as mentioned previously, a healthy elderly may also not present any signs of risk. Regarding this strong correlation, one way to guarantee that the developed algorithm is really distinguishing between people who had risk of falling or not would be, beyond a comparison between young adult subjects and elderly subjects, to have a greater sample of elderly with representation of both classes of risk (i.e., elderly with risk and elderly with no risk).

The main objective of this thesis was to develop a less expensive and easy to set up system in which fall risk could be quantitatively assessed. For this purpose, temporal and gait parameters were automatically extracted from individuals performing the TUG test and walking activity. Those parameters revealed to be promising fall risk indicators. Most of these parameters are not usually measured in a clinical assessment and so this is a way of providing more objective and detailed information to physio-

therapists, in order to help them to pursue treatment options to prevent elderly from falling in the future.

6.2 Future Work

There are some improvements and future work that could be added to this project. First, although some important personal information was obtained from the participants through a questionnaire, it would be beneficial, in addition to asking their history of falls in the past year, to also inquire what caused them to fall. This complementary information could help to understand if a given fall was an one-time situation or a situation that requires more attention from clinicians.

Second, this thesis only focused on acquiring video sequences from a sagittal/lateral view point and so a future development could be the inclusion of frontal view sequences, which might contribute with other reliable fall risk indicators, such as step width, for example.

Finally, the next step would be to collect a larger and diverse sample of elderly subjects with different classes of risk — none, low and high — and then to be able to distinguished them with the proposed system. To perform this classification, fall risk indicators and data inquired from questionnaire could work as input predictors to algorithms of machine learning.

References

[1] While A. "Falls and older people: Understanding why people fall". In: *British journal of community nursing* 25.4 (2020), pp. 173–177.

[2] Voermans N. et al. "Why old people fall (and how to stop them)". In: *Practical neurology* 7.3 (2007), pp. 158–171.

[3] World Health Organization. *Global Report on Falls Prevention in Older Age*. 2008. URL: https://www.who.int/publications/i/item/9789241563536 (visited on 12/17/2020).

[4] Rajagopalan R., Litvan I., and Jung T. "Fall Prediction and Prevention Systems: Recent Trends, Challenges, and Future Research Directions". In: *Sensors* 17.11 (2017), p. 2509.

[5] Johns Hopkins Medicine. *Falls Cost U.S. Hospitals $34 billion in Direct Medical Costs*. 2008. URL: https://www.johnshopkinssolutions.com/article/falls-cost-u-s-hospitals-30-billion-in-direct-medical-costs/ (visited on 12/10/2021).

[6] Igual R., Medrano C., and Inmaculada I. "Challenges, issues and trends in fall detection systems". In: *BioMedical Engineering OnLine* 12.1 (2013), p. 66.

[7] Maki E. B. and McIlroy E. W. "Postural Control in the Older Adult". In: *Clinics in Geriatric Medicine* 12.4 (1996), pp. 635–658.

[8] Pereira C., Baptista F., and Infante P. "Men Older than 50 Yrs Are More Likely to Fall than Women Under Similar Conditions of Health, Body Composition, and Balance". In: *American Journal of Physical Medicine & Rehabilitation* 92.12 (2013), pp. 1095–1103.

[9] Horlings C. et al. "A weak balance: the contribution of muscle weakness to postural instability and falls". In: *Natural Clinical Pratice Neurology* 4.9 (2008), pp. 504–515.

[10] Lecompte E. "Balance improvement of a humanoid robot while walking". MA thesis. École polythecnique de Louvain (EPL), 2017.

[11] Collett J. et al. "Insights into gait disorders: Walking variability using phase plot analysis, Huntington's disease". In: *Gait & Posture* 40.4 (2014), pp. 694–700.

[12] Esser P. et al. "Insights into gait disorders: Walking variability using phase plot analysis, Parkinson's disease". In: *Gait & Posture* 38.4 (2013), pp. 648–652.

[13] Borel L. and Alescio-Lautier B. "Posture and cognition in the elderly: Interaction and contribution to the rehabilitation strategies". In: *Neurophysiologie Clinique/Clinical Neurophysiology* 44.1 (2014), pp. 95–107.

[14] Tencer A. "Biomechanics of Falling". In: *Mayo Clinic Proceedings. Mayo Clinic* 80.7 (2005), pp. 847–848.

[15] Monaco V. et al. "An ecologically-controlled exoskeleton can improve balance recovery after slippage". In: *Scientific Reports* 7.1 (2017), p. 46721.

REFERENCES

[16] Boyd J. and Little J. J. "Biometric Gait Recognition". In: *Proceedings of the 1st International Conference on Advanced Studies in Biometrics*. Vol. 3161. Alghero, Italy, 2003, pp. 19–42.

[17] Vaughan L. C., Davis L. B., and O'Connor C. J. *Dynamics of Human Gait*. 2nd ed. Cape Town, South Africa: Kiboho Publishers, 1992.

[18] Kharb A. et al. "A review of gait cycle and its parameters". In: *International Journal of Computational Engineering and Management* 13 (2011).

[19] Pirker W. and Katzenschlager R. "Gait disorders in adults and the elderly: A clinical guide". In: *Wiener klinische Wochenschrift* 129.3-4 (2016), pp. 81–95.

[20] Chen S. et al. "Toward Pervasive Gait Analysis With Wearable Sensors: A Systematic Review". In: *IEEE Journal of Biomedical and Health Informatics* 20.6 (2016), pp. 1521–1537.

[21] Muro A., Zapirain B., and Mendez-Zorrilla A. "Gait Analysis Methods: An Overview of Wearable and Non-Wearable Systems, Highlighting Clinical Applications". In: *Sensors* 14.2 (2014), pp. 3362–3394.

[22] Haas D. *GAITRite - The Gold Standard in Gait Analysis for 26years*. 2016. URL: `https://www.gaitrite.com/` (visited on 12/17/2020).

[23] APDM Wearable Technologies. *ERT Clinical*. 2020. URL: `https://www.apdm.com/wearable-sensors/` (visited on 12/17/2020).

[24] Nandy A. et al. "Gait identification using component based gait energy image analysis". In: *2014 International Conference on Signal Propagation and Computer Technology*. Ajmer, India, 2014, pp. 380–385.

[25] Gandomkar Z. and Bahrami F. "Method to classify elderly subjects as fallers and non-fallers based on gait energy image". In: *Healthcare Technology Letters* 1.3 (2014), pp. 110–114.

[26] Ortells J., Herrero M., and Mollineda R. "Vision-based gait impairment analysis for aided diagnosis". In: *Medical & Biological Engineering & Computing* 56.9 (2018), pp. 1553–1564.

[27] Vicon Motion Systems Limited. *What is Motion Capture*. URL: `https://www.vicon.com/about-us/what-is-motion-capture` (visited on 12/17/2020).

[28] Sant'Anna A. and Wickström N. "A Symbol-Based Approach to Gait Analysis From Acceleration Signals: Identification and Detection of Gait Events and a New Measure of Gait Symmetry". In: *IEEE Transactions on Information Technology in Biomedicine* 14.5 (2010), pp. 1180–1187.

[29] Vicon Motion Systems Limited. *OptiTrack*. 2020. URL: `https://optitrack.com/` (visited on 12/17/2020).

[30] Visual Effects Society. *What MOCAP suit suits you?* 2020. URL: `https://www.vfxvoice.com/what-mocap-suit-suits-you/` (visited on 12/17/2020).

[31] Thuc H., Tuan P., and Hwang J. "An effective video-based model for fall monitoring of the elderly". In: *2017 International Conference on System Science and Engineering (ICSSE)*. 2017, pp. 48–52.

[32] Mar Systems Ltd. *Markerless Motion Capture - How it works?* 2020. URL: `https://www.mar-systems.co.uk/motionmetrix_3d-running-analysis/markerless-motion-capture/` (visited on 12/17/2020).

[33] Stuberg W. et al. “Comparison of a Clinical Gait Analysis Method Using Videography and Temporal-Distance Measures with 16-mm Cinematography”. In: *Physical therapy* 68.8 (1988), pp. 1221–1225.

[34] Perell-Gerson K. et al. “Fall Risk Assessment Measures: An Analytic Review”. In: *The journals of gerontology. Series A, Biological sciences and medical sciences* 56.12 (2002), pp. M761–M766.

[35] Dias C. M. and Ferreira P. “Escalas de avaliação de risco de quedas”. In: *Revista de Enfermagem Referência* IV Série.2 (2014), pp. 153–161.

[36] Morse J., Morse R., and Tylko S. “Development of a Scale to Identify the Fall-Prone Patient”. In: *Canadian Journal on Aging / La Revue canadienne du vieillissement* 8.04 (1989), pp. 366–377.

[37] Oliver D. et al. “Development and evaluation of evidence based risk assessment tool (STRATIFY) to predict which elderly inpatients will fall: Case-control and cohort studies”. In: *BMJ (Clinical research ed.)* 315.7115 (1997), pp. 1049–1053.

[38] Podsiadlo D. and Richardson S. “The timed ”Up & Go”: a test of basic functional mobility for frail elderly persons”. In: *Journal of the American Geriatrics Society* 39.2 (1991), pp. 142–148.

[39] Berg K. “Balance and its measure in the elderly: a review”. In: *Physiotherapy Canada* 41.5 (1989), pp. 240–246.

[40] Tinetti E. M. “Performance-oriented assessment of mobility problems in elderly patients”. In: *Journal of the American Geriatrics Society* 34.2 (1986), pp. 119–126.

[41] Barry E. et al. “Is the Timed Up and Go test a useful predictor of risk of falls in community dwelling older adults: A systematic review and meta- analysis”. In: *BMC geriatrics* 14.1 (2014), p. 14.

[42] Skrba Z. et al. “Objective real-time assessment of walking and turning in elderly adults”. In: *2009 Annual International Conference of the IEEE Engineering in Medicine and Biology Society*. Hilton Minneapolis, Minnesota, 2009, pp. 807–810.

[43] Lohmann O., Luhmann T., and Hein A. “Skeleton Timed Up and Go”. In: *2012 IEEE International Conference on Bioinformatics and Biomedicine*. Philadelphia, USA, 2012, pp. 1–5.

[44] Wang F. et al. “Quantitative analysis of 180 degree turns for fall risk assessment using video sensors”. In: *2011 Annual International Conference of the IEEE Engineering in Medicine and Biology Society*. Boston,USA, 2011, pp. 7606–7609.

[45] Frenken T. et al. “Performing gait analysis within the timed up & go assessment test: Comparison of aTUG to a marker-based tracking system”. In: *Informatics for health & social care* 39.3-4 (2014), pp. 232–248.

[46] Romeo L. et al. “Vision-based Assessment of Balance Control in Elderly People”. In: *2020 IEEE International Symposium on Medical Measurements and Applications (MeMeA)*. Bari,Italy, 2020, pp. 1–6.

[47] Gervásio M. F. et al. “Medidas temporoespaciais indicativas de quedas em mulheres saudáveis entre 50 e 70 anos avaliadas pela análise tridimensional da marcha”. In: *Fisioterapia e Pesquisa* 23.4 (2016), pp. 358–364.

[48] Kingetsu H. et al. “Video-based Fall Risk Detection System for the Elderly”. In: *2019 IEEE 1st Global Conference on Life Sciences and Technologies (LifeTech)*. Osaka,Japan, 2019, pp. 148–149.

[49] Makihara Y. et al. “Gait Recognition: Databases, Representations, and Applications”. In: 2015.

[50] Sulaiman S. et al. “Human Silhouette Extraction Using Background Modeling and Subtraction Techniques”. In: *Information Technology Journal* 7.1 (2008), pp. 155–159.

[51] Nguyen T., Huynh H., and Meunier J. “Extracting silhouette-based characteristics for human gait analysis using one camera”. In: *Proceedings of the Fifth Symposium on Information and Communication Technology*. Hanoi, Vietnam, 2014, pp. 171–177.

[52] Han J. and Bhanu B. “Individual recognition using gait energy image”. In: *IEEE Transactions on Pattern Analysis and Machine Intelligence* 28.2 (2006), pp. 316–322.

[53] Verlekar T. T. “Gait Analysis in Unconstrained Environments”. PhD thesis. Instituto Superior Técnico, 2019.

[54] Wagg K. D. and Nixon S. M. “On automated model-based extraction and analysis of gait”. In: *Sixth IEEE International Conference on Automatic Face and Gesture Recognition, 2004. Proceedings.* Seoul,Korea, 2004, pp. 11–16.

[55] Wang L. et al. “Fusion of static and dynamic body biometrics for gait recognition”. In: *IEEE Transactions on Circuits and Systems for Video Technology* 14.2 (2004), pp. 149–158.

[56] GitHub. *OpenPose Doc - Output*. 2020. URL: `https://github.com/CMU-Perceptual-Computing-Lab/openpose/` (visited on 04/12/2021).

[57] Loureiro J. “Using Deep Learning for Gait Abnormality Classification”. MA thesis. Instituto Superior Técnico, 2019.

[58] Ng K. et al. “Measuring Gait Variables Using Computer Vision to Assess Mobility and Fall Risk in Older Adults With Dementia”. In: *IEEE Journal of Translational Engineering in Health and Medicine* 8 (2020), p. 2100609.

[59] Hausdorff J. “Gait Variability: Methods, Modeling and Meaning”. In: *Journal of neuroengineering and rehabilitation* 2.1 (2005), p. 19.

[60] Rubenstein L. et al. “Validating an evidence-based, self-rated fall risk questionnaire (FRQ) for older adults”. In: *Journal of Safety Research* 42.6 (2011), pp. 493–499.

[61] Cao Z. et al. “OpenPose: Realtime Multi-Person 2D Pose Estimation Using Part Affinity Fields”. In: *IEEE Transactions on Pattern Analysis and Machine Intelligence* 43.1 (2021), pp. 172–186.

[62] Otsu N. “A Threshold Selection Method from Gray-Level Histograms”. In: *IEEE Transactions on Systems, Man, and Cybernetics* 9.1 (1979), pp. 62–66.

[63] Beerse M., Lelko M., and Wu J. “Biomechanical analysis of the timed up-and-go (TUG) test in children with and without Down syndrome”. In: *Gait & Posture* 68 (2019), pp. 409–414.

[64] Zago M. et al. “3D Tracking of Human Motion Using Visual Skeletonization and Stereoscopic Vision”. In: *Frontiers in Bioengineering and Biotechnology* 8.5 (2020), p. 181.

[65] Beyea J. et al. “Convergent Validity of a Wearable Sensor System for Measuring Sub-Task Performance during the Timed Up-and-Go Test”. In: *Sensors* 17.4 (2017), p. 934.

[66] Rochon J., Gondan M., and Kieser M. “To test or not to test: Preliminary assessment of normality when comparing two independent samples”. In: *BMC medical research methodology* 12.1 (2012), p. 81.

[67] Wilcoxon F. “Individual Comparisons by Ranking Methods”. In: *Biometrics Bulletin* 1.6 (1945), pp. 80–83.

Appendix A

Pre-Acquisition Questionnaire

Questionário

Estudo: Avaliação de risco acrescido de queda na população idosa

1. **IDADE**

   Indique a sua idade: _____

2. **SEXO**

   Selecione o seu sexo: **Feminino** ☐ **Masculino** ☐

3. **PESO**

   Indique o seu peso (kg): _____

4. **ALTURA**

   Indique a sua altura (cm): _____

5. **HISTÓRICO DE QUEDAS**

   5.1. Nos últimos 12 meses, registou alguma queda? **Sim** ☐ **Não** ☐

   5.2. Se Sim, quantas vezes? _____

6. **DISPOSITIVO AUXILIAR DE MARCHA**

   6.1. No seu dia-a-dia, recorre a algum dispositivo que o ajude a andar?

   Sim ☐ **Não** ☐

   6.2. Se Sim, qual? _____

7. **PATOLOGIAS MOTORAS**

   7.1. Já lhe foi diagnosticado alguma patologia que afete a sua capacidade motora? **Sim** ☐ **Não** ☐

   7.2. Se sim, qual? _____

Figure A.1: Example of questions inquired to both populations before acquisitions started.

Appendix B

Pre-Acquisition Questionnaire Answers

	Age	Sex	Weight	Height	History of Falls	Walking Aid	Motor Diseases
C01	21	F	68	169	-	-	-
C02	22	F	56	179	-	-	-
C03	22	M	78	173	-	-	-
C04	21	F	81	172	-	-	-
C05	23	F	65	165	-	-	-
C06	21	F	51	157	-	-	-
C07	22	F	64	165	-	-	-
C08	23	M	68	179	-	-	-
C09	20	F	60	157	-	-	-
C10	23	F	90	174	-	-	-
C12	20	F	51	163	-	-	-
C13	23	F	62	165	-	-	-
C14	21	F	62	160	-	-	-
C15	23	F	83	170	-	-	-
C16	21	F	45	153	-	-	-
C17	23	F	61	163	-	-	-
C18	24	F	65	162	-	-	-
C20	20	M	80	185	-	-	-
C21	28	M	82	180	-	-	-
C22	23	M	70	178	-	-	-
C23	23	M	68	180	-	-	-
C24	22	M	76	171	-	-	-
C25	22	M	104	175	-	-	-
C26	20	F	58	155	-	-	-
C27	22	F	76	168	-	-	-
C28	21	F	55	158	-	-	-
C29	23	F	66	178	-	-	-

Table B.1: Questionnaire answers for the control group composed of 27 young adult subjects.

	Age	Sex	Weight	Height	History of Falls	Walking Aid	Motor Diseases
E01	75	F	60	165	-	Crutches	-
E02	59	F	100	167	-	Crutches	-
E03	75	F	78	154	-	-	Gonarthrosis
E04	65	F	74	170	2	-	-
E05	80	F	70	162	2	-	-
E06	87	F	68	153	1	-	-

Table B.2: Questionnaire answers for the elderly group composed of 6 subjects.

Appendix C

Informed Consent Form

Ciências ULisboa | Comissão de Ética para a Recolha e Protecção de Dados de Ciências

Formulário de Consentimento Informado

V2, 1-2-2018

PROJECTO: Avaliação de risco acrescido de queda em idosos através da captura de vídeo durante a marcha

INVESTIGADOR RESPONSÁVEL: Nuno Matela

Agradecemos o seu interesse e colaboração neste estudo.
Por favor, preencha o formulário que se segue. Receberá uma cópia quando sair.

1. Confirmo que li e compreendi o folheto informativo associado ao projecto. ☐
2. Foi-me dada a oportunidade de ler e considerar a informação apresentada, e fazer perguntas, as quais foram respondidas de forma satisfatória. ☐
3. Compreendo que a minha participação é voluntária e que sou livre de desistir do estudo em qualquer altura, sem ter que dar quaisquer explicações e sem quaisquer consequências. ☐
4. Compreendo que os dados recolhidos durante o estudo possam ser do conhecimento dos membros da equipa de investigação, sempre que necessário para o estudo. Autorizo que os membros da equipa tenham acesso a esses dados. ☐
5. Compreendo que, caso esta investigação venha a ser publicada, todos os dados serão mantidos anónimos e nenhuma informação será identificável como sendo minha. ☐
6. Gostaria que me fosse enviado o relatório final do estudo. ☐

   O meu endereço de e-mail é: _____
7. Gostaria de ser contactado para o endereço acima acerca de sessões ou estudos adicionais relacionados com este estudo. ☐
8. Declaro que não comuniquei nenhuma razão potencial de qualquer natureza que constitua um eventual factor de risco para a minha saúde ou integridade física. ☐
9. Declaro que participo neste estudo sem qualquer remuneração ou contrapartida, para além do ressarcimento das despesas em que tiver incorrido. ☐
10. Declaro que aceito que as minhas atividades sejam gravadas em vídeo, incluindo a cara. ☐
11. **Declaro que tomo a minha decisão de forma inteiramente livre.** ☐
12. **Concordo em participar neste estudo.** ☐

_____ _____ ___/___/___
Nome do Participante Assinatura Data

Sou da opinião que o participante compreendeu os aspectos relevantes da informação fornecida e está apto a tomar uma decisão informada.

_____ ___/___/___
Assinatura do Investigador Responsável Data

Faculdade de Ciências, Universidade de Lisboa | Campo Grande, 1749-016 Lisboa – Portugal | direccao@ciencias.uLisboa.pt | www.ciencias.uLisboa.pt

Figure C.1: Example of the Informed Consent form assigned before acquisitions by the participants included in this study.